Adaptive Thresholding of the GIP Statistic to Remove Ground Target Returns from the Training Data for STAP Applications

Christopher M. Teixeira, Jameson S. Bergin, and Paul M. Techau
Information Systems Laboratories, Inc.
8130 Boone Blvd. Ste. 500
Vienna, VA 22182
email: cmt@isl-inc.com
email: jsb@isl-inc.com
email: pmt@isl-inc.com

Abstract This paper presents an adaptive thresholding algorithm that can be used in conjunction with the multi-pass GIP-based editing method to adaptively eliminate ground moving target returns ("non-homogeneities") from the training data used for space-time adaptive processing (STAP) applications, such as adaptive radars. The algorithm exploits a property of the generic structure of the ordered GIP statistic, the origins of which have been theoretically developed by the authors, and a single adjustable parameter related to the Type I error of incorrectly excising target-free training data to adaptively determine the thresholds for excising target-contaminated training data. An iterative application of the method improves the distinction between non-homogeneities and background clutter, which increases the number of target-contaminated training bins excised. Moreover, the editing method has been extended to reduced degree-of-freedom (DoF) STAP implementations such as multi-bin post-Doppler STAP. As a consequence, the method is practically implementable for realistic scenarios with very limited *a priori* knowledge (i.e., only the number of DoFs is required).

The resulting STAP performance improvement with the new technique is demonstrated by applying it to both high-fidelity, site-specific, high-traffic density simulation data with a realistic radar waveform and experimental (MCARM) data. Performance metrics include SINR Loss, P_d vs. P_{fa} curves, and association of target detections with road locations (for the experimental data). Results with the simulated data using the developed GIP-editing technique essentially recover the target detection performance of clutter-only training data when an ideal waveform (i.e., no range sidelobes) is used. The presence of a realistic waveform, as might be used with pulse compression, produces range sidelobes that degrade the performance of the editing algorithm as a function of range sidelobe level due to reduced sensitivity. However, significant improvement in target detection performance is still obtained relative to no-editing. Analysis of the experimental MCARM data with the developed GIP-editing technique indicates that the number of detections is about doubled, relative to the unedited results, and that they are also better associated with known road locations in the scenario. A preliminary analysis of the computational complexity of the editing algorithm is also performed.

Report Documentation Page

Form Approved
OMB No. 0704-0188

1. REPORT DATE	2. REPORT TYPE	3. DATES COVERED
20 DEC 2004	**N/A**	**-**

4. TITLE AND SUBTITLE
Adaptive Thresholding of the GIP Statistic to Remove Ground Target Returns from the Training Data for STAP Applications

5a. CONTRACT NUMBER
5b. GRANT NUMBER
5c. PROGRAM ELEMENT NUMBER

6. AUTHOR(S)

5d. PROJECT NUMBER
5e. TASK NUMBER
5f. WORK UNIT NUMBER

7. PERFORMING ORGANIZATION NAME(S) AND ADDRESS(ES)
Information Systems Laboratories, Inc. 8130 Boone Blvd. Ste. 500 Vienna, VA 22182

8. PERFORMING ORGANIZATION REPORT NUMBER

9. SPONSORING/MONITORING AGENCY NAME(S) AND ADDRESS(ES)

10. SPONSOR/MONITOR'S ACRONYM(S)

11. SPONSOR/MONITOR'S REPORT NUMBER(S)

12. DISTRIBUTION/AVAILABILITY STATEMENT
Approved for public release, distribution unlimited

13. SUPPLEMENTARY NOTES
See also, ADM001741 Proceedings of the Twelfth Annual Adaptive Sensor Array Processing Workshop, 16-18 March 2004 (ASAP-12, Volume 1)., The original document contains color images.

14. ABSTRACT

15. SUBJECT TERMS

16. SECURITY CLASSIFICATION OF:			17. LIMITATION OF ABSTRACT	18. NUMBER OF PAGES	19a. NAME OF RESPONSIBLE PERSON
a. REPORT	b. ABSTRACT	c. THIS PAGE			
unclassified	**unclassified**	**unclassified**	**UU**	**34**	

Standard Form 298 (Rev. 8-98)
Prescribed by ANSI Std Z39-18

ADAPTIVE THRESHOLDING OF THE GIP STATISTIC TO REMOVE GROUND TARGET RETURNS FROM THE TRAINING DATA FOR STAP APPLICATIONS

Christopher M. Teixeira, Jameson S. Bergin, Paul M. Techau

cmt@isl-inc.com, jsb@isl-inc.com, pmt@isl-inc.com

Information Systems Laboratories, Inc.

8130 Boone Boulevard Suite 500, Vienna, VA 22182 USA

Abstract - **An adaptive thresholding algorithm is presented that can be used in conjunction with the multi-pass generalized inner product (GIP)-based editing method to eliminate non-homogeneities from the training data used for space-time adaptive processing (STAP) applications such as adaptive radars. The algorithm exploits a property of the generic structure of the ordered GIP statistic along with a single user-specified parameter related to the Type I error of incorrectly excising target-free training data to adaptively determine the thresholds for excising target-contaminated training data. The performance of the method is demonstrated using both high-fidelity site-specific simulated data with both ideal and realistic waveforms as well as measured data from the Multi-Channel Airborne Radar Measurement (MCARM) experiment.**

I. INTRODUCTION

The deleterious impact of non-homogeneous training data on covariance estimation and space-time adaptive processing (STAP) [1] performance for real-world airborne ground-moving target indicator (GMTI) radar data has been widely reported [2-6]. The main consequences are under-nulled clutter, unintentional cancellation of targets of interest, and reduced detection performance. This has led to the development of improved training data selection techniques that seek to edit out bins that are sufficiently non-homogeneous from the bulk of the training data. Such non-homogeneity detection (NHD) methods may be either data dependent or data independent. In this paper we focus on a data-dependent technique based on the generalized inner-product (GIP) [3-4].

The GIP, γ, is a scalar statistic that incorporates both power and phase information of the data [4]. It is defined as $\gamma = \mathbf{x}^H\mathbf{R}^{-1}\mathbf{x}$ where $\mathbf{x}$ is the $MN \times 1$ radar data (M = number of pulses, N = number of channels), and $\mathbf{R}$ is the interference-plus-noise covariance matrix, which, in practice, must be estimated from training data. "Large" values of this statistic, equivalent to the power of the whitened data vector, correspond to nonhomogeneities (e.g. ground-movers) and should be excised. However, the presence of targets in the training data corrupts the covariance estimate in the GIP as it does the STAP weight calculation, resulting in underprediction of the GIP relative to its true value (i.e. using the ideal covariance). This increases the difficulty of distinguishing between targets and clutter [6]. To address this, an iterative technique (called the "multi-pass" algorithm [3]) has been developed whereby the reduced training set is used to recompute the GIP and the process of excision is repeated until convergence of the GIP statistic as a function of range is achieved.

Unfortunately, it is not clear how to define what values of GIP are too "large," i.e. what are the thresholds for excision? A survey of previous work reveals two basic approaches. First, a prescribed number of bins may be removed corresponding to the outlier values of GIP [3, 7]. Improvement results but it is not clear how to optimally choose the number of bins to remove. A second approach [7, 8] is to use statistical properties of the GIP derived from its probability distribution function (pdf) to set the thresholds. This method works well if the assumed pdf accurately represents the data. However, the presence of inhomogeneous training data and the use of techniques to compensate for the absence of adequate training data, such as diagonal loading, can significantly alter this pdf, making the use of deterministic limits from theoretical considerations inaccurate for practical use. The use of realistic waveforms, which produce radar return range sidelobes, will tend to also adversely affect this editing process.

This paper presents an adaptive thresholding algorithm that can be used in conjunction with the multi-pass GIP-based editing method [3] to eliminate ground-moving target returns from the training data used for STAP applications. The algorithm does not require knowledge of the pdf of the GIP, nor an *a priori* estimate of the number of targets to be removed. The algorithm exploits a property of the generic structure of the ordered GIP statistic along with a single user-specified parameter related to the Type I error of incorrectly excising target-free training data to adaptively determine the thresholds for excising target-contaminated training data. The performance of the method is demonstrated using both high-fidelity site-specific simulated data as well as measured data from the MCARM experiment [9].

In Section II, the method is described and the theoretical origins of the GIP properties exploited by the algorithm are

---

Presented at the 2004 Adaptive Sensor Array Processing Workshop, Lexington, MA, 16-18 March, 2004.

This work was sponsored under Army Contract DAAH01-02-C-R177.

Approved for Public Release. Distribution Unlimited.

presented. Extensions to reduced degree-of-freedom (DoF) STAP implementations such as multi-bin post-Doppler STAP [10] are also described. Section III presents results using site-specific simulated data. Performance metrics include SINR loss and P_d vs. P_{fa} curves. In Section IV, results with experimental MCARM data are reported. Section V summarizes the findings and outlines areas for further research.

II. Thresholding Algorithm and Theory

The adaptive thresholding algorithm is illustrated by applying it to the first data cube released under DARPA's Knowledge-Aided Sensor Signal Processing and Expert Reasoning (KASSPER) program [11]. This data, from the KASSPER 2002 Workshop [12], simulates an L-band radar with parameters similar to the system used under the MCARM program [9] and includes site-specific clutter computed using digital terrain elevation data (DTED). Thus this data set represents a generally heterogeneous clutter environment. Additional real-world elements of the simulation include array calibration errors on the order of 5-10 degrees, clutter discretes, platform crab, internal clutter motion (ICM), and a significant number of ground moving targets in the radar mainbeam. The simulated system uses 32 pulses and 11 channels for 352 total DoFs. Details of the simulation technique used and additional radar parameters are provided in [12].

Figure 1 demonstrates the adaptive thresholding process with the GIP statistic computed using both the ideal covariance and the sample covariance (using 200 range bins, 100 on either side of the bin under test, and 0 dB of diagonal loading relative to the white thermal noise), as a function of one-way radar range for the KASSPER data. Other researchers have previously analyzed the rank-ordering of the resulting GIP statistic [3, 4]. We observe that the rank-ordered GIP has a broad "central" region that is nearly linear and find the best-fit line to this region. The upper and lower thresholds are then determined to be the points that deviate by a prescribed relative fraction, α, from this straight line. Figure 1 illustrates that while the GIP profile computed using the sample covariance is significantly reduced in comparison with the ideal covariance profile due to the contaminating effect of targets in the training data, the sorted profiles have very similar structure. Repeated application of the iterative editing process improves the number of target-contaminated bins that are excised. In practice, we have found that typically at most five GIP iterations are required to recover the performance of the sampled result using clutter-only data and an ideal waveform.

A. Ordered Statistic Theory

Two key theoretical issues related to the algorithm are: 1) the robustness of the extended linear region in the sorted GIP graph, and 2) the relationship between the value of α and the properties of the GIP statistic.

To investigate the first of these issues, the normalized GIP statistic was examined, $\gamma' = \gamma/Q = (\mathbf{x}^H\mathbf{R}^{-1}\mathbf{x})/Q$, where $Q = NM$ is the total number of DoFs. In the following we present highlights of the derivation while details may be

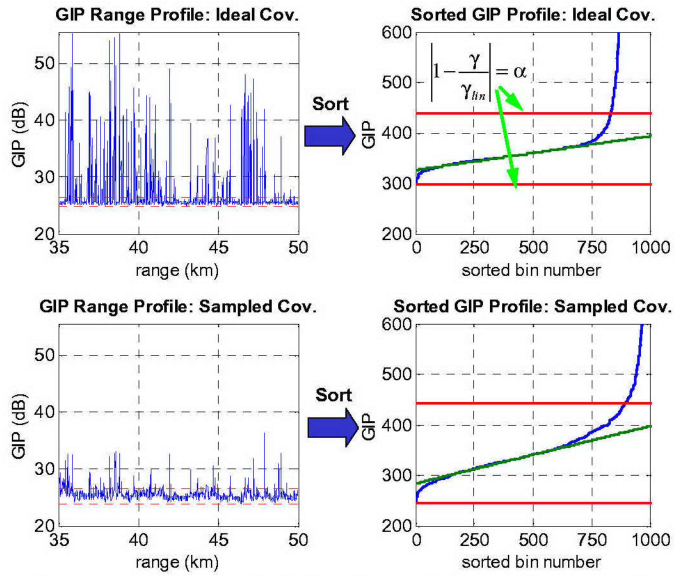

Fig. 1. Comparison of ideal and sampled covariance results for the adaptive thresholding algorithm.

found in [15]. Assuming target-free Gaussian data, the normalized GIP has a modified gamma pdf [8] and a resulting cumulative distribution function (cdf) $F(\gamma')$ that may be computed explicitly but is not expressible in closed form.

If p samples of the normalized GIP are acquired and sorted in ascending order, the pdf of the rth sample ($1 \le r \le p$) in this ordered list (the "rth order statistic") may be computed using standard techniques [13].

The moments of the rth order statistic, particularly the mean and variance, are of interest. The qth moment can be expressed in terms of the inverse of the cdf $F^{-1}(t)$ called the quantile function

$$E[(\gamma'_r)^q] = \int_0^\infty (\gamma_r)^q f_{\gamma,r}(\gamma')d\gamma' = \int_0^1 [F^{-1}(t)]^q f_\beta(t)dt \qquad (1)$$

where the transformation $t = F(\gamma')$ has been made and $f_\beta(t)$ is the standard beta pdf [14]. Analytical evaluation of these moments are difficult since a closed form expression for the quantile function of the normalized gamma pdf does not exist. Instead, a Taylor expansion of the normalized gamma cdf was formed around the most probable value of γ', $\gamma'_{max} = 1 - 1/Q$, and it was observed that the second order term in the expansion vanishes if $Q > 1$. Thus, around the most probable value of γ', a good approximation to the quantile function may be found by inverting the expansion of the cdf to first order

$$F^{-1}(t) = \gamma' \approx \frac{1}{P_\gamma(\gamma'_{max})}t + \gamma'_{max} - \frac{F_0(\gamma'_{max})}{P_\gamma(\gamma'_{max})} \qquad (2)$$

where $P_{\gamma'}(\gamma'_{max}) \approx \sqrt{Q/(2\pi)}$ from the normalized GIP pdf and $F_0(\gamma'_{max})$ is the zeroth-order term in the Taylor expansion of the cdf evaluated at the most probable value of γ'.

Substituting (2) into (1) and using general results for polynomial moments of the beta pdf [14] allows approximate eval-

uation of the moments of the rth order statistic. For example, an approximation to the mean can be shown to be

$$\mu_r \approx F^{-1}\left(\frac{r}{p+1}\right) \approx \sqrt{\frac{2\pi}{Q}}\left(\frac{r}{p+1}\right) + 1 - \sqrt{\frac{\pi}{2Q}} = \mu_{r,\,lin}. \quad (3)$$

This result demonstrates that the mean of the rth order statistic of the normalized GIP around the most probable value is linearly related to the order statistic number r. The absence of the second order term in the expansion of the cdf $F(\gamma')$ explains the broad, central linear region that we exploit in the GIP editing algorithm. The excellent accuracy and robustness of these approximations, for both the linear region using $\mu_{r,\,lin}$ and for the entire domain using $\mu_r \approx F^{-1}(r/(p+1))$, has been demonstrated with the KASSPER data using the ideal covariance and a single trial of data, see Figure 2. We note that this simulated data is non-Gaussian due to the implementation of the ICM model [12] and heterogeneous terrain.

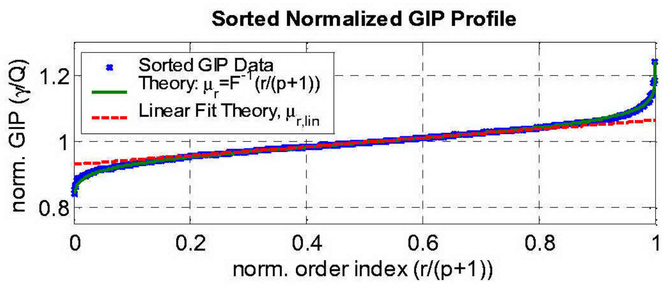

Fig. 2. Comparison of sorted GIP computed from the KASSPER data to theory (3).

The thresholds for editing are determined as the range bins corresponding to the order statistics that deviate from the linear approximation by a given fractional error

$$\left|\frac{\mu_r - \mu_{r,\,lin}}{\mu_{r,\,lin}}\right| > \alpha. \quad (4)$$

It is assumed that any ordered statistic that exceeds this fractional deviation from the central linear region (assumed to contain "homogeneous" data) contains a target and should be excised. In [15], guidance for choosing α is provided in terms of a function with the number of DoFs and desired level of statistical Type I error as inputs. Typical values of α range from 0.15 for large full-DoF scenarios (as in Figure 1) to 0.25 for small reduced-DoF situations.

B. Reduced-DoF STAP Implementation

For many systems it may be impractical to use full-DoF STAP for reasons of computational complexity and the absence of sufficient sample support for covariance estimation. In such situations, it is desirable to reduce the number of DoFs to a manageable number while minimizing any loss in performance relative to the full-DoF formulation. The adaptive thresholding algorithm may be straightforwardly applied to such reduced-DoF formulations by simply computing the GIP with the reduced-DoF variables and then applying the same thresholding procedure to the resulting GIP.

An example of a reduced-DoF technique is extended factored or multi-bin post-Doppler STAP [10]. With this method, the number of spatial DoFs are preserved while the temporal DoFs are reduced to a specified number of (typically orthogonal) Doppler bins for each cell under test. The thresholding algorithm may be applied to the GIP results for each Doppler bin as a function of range as described before. As a consequence, the number of contaminating targets in the training data is now a function of Doppler bin. To further reduce the potential of target contamination, a "master list" for each bin is compiled as the intersection of allowed range bins amongst the multiple Doppler bins used for the DoF reduction for the specified cell under test.

III. Simulation Results

In this section, the performance of the multi-pass adaptive thresholding algorithm when applied to the previously described high-fidelity site-specific KASSPER simulated L-band datacube is analyzed in conjunction with both full-DoF and reduced-DoF multi-bin post-Doppler STAP implementations. The full-DoF (352 DoFs) implementation used 200 local samples ($K = 200$) and 0 dB of diagonal loading relative to the white thermal noise to estimate the covariance. Two reduced-DoF implementations were examined using 3 and 5 post-Doppler bins (33 and 55 DoFs, respectively). A training sample size of $K = 2Q$ range bins were used to form the sampled covariance in both cases (i.e. 66 and 110 samples, respectively) with 0 dB of diagonal loading. The same training strategies were used for both the GIP pre-processing and STAP steps. The value of the thresholding fraction was chosen to be $\alpha = 0.15$ for the full-DoF case and increased to $\alpha = 0.20$ for the reduced-DoF cases. The GIP processing step was repeated until the training list had converged for each case (approximately 5 iterations).

Elsewhere it has been shown that the GIP-editing process is effective in removing high SNR targets from the training data for both full- and reduced-DoF STAP implementations with this data [15]. A consequence of this editing step is an improvement in the ratio of signal-to-interference-plus-noise to signal-to-noise (SINR loss). This is demonstrated in Figure 3 where the SINR loss as a function of range and Doppler for all three cases are shown. Note that the mainbeam clutter notch is located at the two-way Doppler shift of ~51 m/s due to the antenna beam being steered away from broadside. The improvement in SINR loss with editing is significant, particularly around the highly contaminated region of 0 m/s Doppler, where the improvement with editing may be as large as 22.5 dB. Other Dopplers where improvement is seen include 90 m/s and 30 m/s (near to the clutter).

To further investigate the benefit of the GIP-editing process, the KASSPER space-time beamformed clutter data was post processed with a median constant false alarm (CFAR) algorithm [16] that employed 100 range bins and a single Doppler bin to compute a background noise level for the beamformer output. The normalized beamformer output was

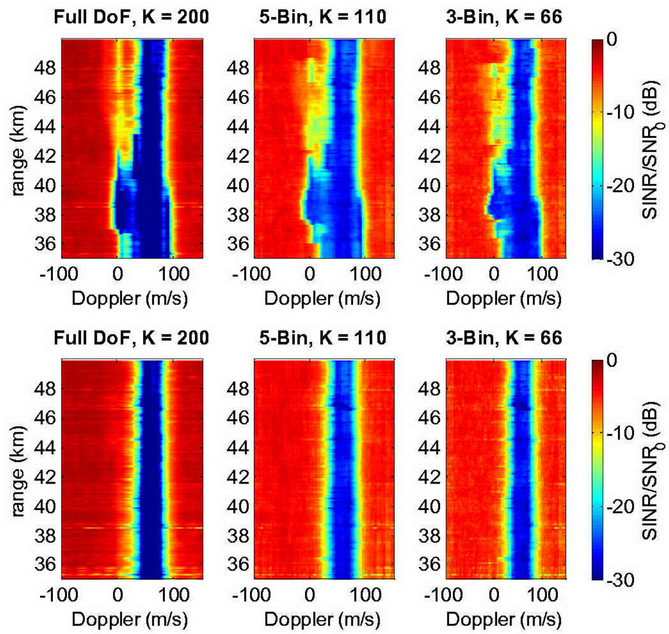

Fig. 3. SINR loss for unedited (top) and GIP-edited (bottom) training data. Left: full-DoF; Middle: 5-Bin post-Doppler; Right: 3-Bin post-Doppler. Two-way Doppler is shown.

thresholded and the number of false alarms was recorded. The sample processing steps were then applied to a series of test targets in all range bins for a specified Doppler shift. The target SNR was set to 25 dB at the closest range bin which represents a radar cross section of approximately 5 dBsm. The target SNR was then reduced versus range using an inverse range to the fourth power rule which resulted in a target SNR of 19 dB at the longest range in the simulation. The number of targets exceeding the thresholds when processed using the same beamformer weights and CFAR normalization was also recorded. P_d vs. P_{fa} curves were then generated using the observed number of false alarms and detections.

Figure 4 shows the P_d vs. P_{fa} curves for a Doppler velocity of 0 m/s (note: clutter at 51 m/s) around which many targets may be found (see Figure 3). The unedited results for all three sampled cases show dramatic degradation relative to the optimal ideal covariance case due to the impact of targets in the training data. However, the GIP-edited results demonstrate significant improvement of Pd relative to the unedited results due to the effective removal of contaminating targets from the training data.

The results presented so far have used an ideal waveform (i.e. a rectangular pulse whose length equals the inverse of the system bandwidth and has infinitely low sidelobes). However, a realistic waveform results in energy leakage (i.e. sidelobes) of the target response in range. An example of this is the compressed linear frequency modulated (LFM) waveform, which was used in this study and is described below. The resulting increased self-contamination of the covariance estimate reduces the value of the GIP making it even more difficult to distinguish non-homogeneities from the background. This

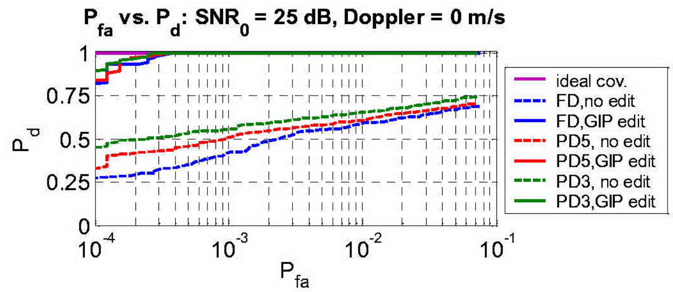

Fig. 4. P_d vs. P_{fa} curves for Doppler velocity 0 m/s. Unedited (dashed) and GIP-edited (solid) training data results for all three cases shown. Full DoF results (FD) use $K = 200$, 5-bin (PD5) results use $K = 110$, and 3-bin (PD3) $K = 66$.

desensitization of the GIP causes fewer target contaminated bins to be edited out and results in degraded performance relative to the edited ideal waveform case.

This effect was investigated using the KASSPER data with the targets reproduced using a compressed LFM waveform with a Taylor pulse compression taper (with nbar=6) and a duty factor of 0.1. Taper sidelobe levels of 20, 25, 30, 35, and 40 dB below the peak response were examined. The previously described 5-bin post-Doppler (K=110) STAP architecture with four guard bins on either side of the cell under test was used. As expected the GIP variation and level with the converged list was seen to increase with reduced sidelobe level. P_d vs. P_{fa} performance results using the median CFAR and the previously described target inject process for all waveforms including ideal are shown in Figure 5. In these results, the clutter contribution is processed with the ideal waveform for all cases while the LFM waveform affects only the targets. Both the unedited and GIP-edited results, presented separately, are seen to degrade with increased sidelobe level. However, except at the largest sidelobe (20 dB) and lowest P_{fa} levels, GIP-editing provides a significant improvement in P_d over no-editing with the LFM waveform. We also note the insensitivity to further improvement as the sidelobe level is reduced below 35 dB.

A potential reason for the loss of performance with GIP-editing at low levels of P_{fa} is that the same level of sample support was used for all cases resulting in some loss of training data locality for the edited cases and a resulting increased sampling error for the covariance estimate. This was confirmed by performing the same analysis using uncontaminated (i.e. clutter-plus-noise-only) training data without and with the GIP-edited training list and the same training strategy. The resulting P_{fa} curves for both were very similar to those using contaminated training data. This indicates that the loss in P_{fa} performance with the edited training list is primarily due to non-locality effects in the training data rather than residual target contamination effects. In the future, we will examine the degree to which this effect is site-specific (i.e. pronounced in areas of significant terrain heterogeneity) and whether it may be mitigated by using sample support reduction techniques (e.g. [22]).

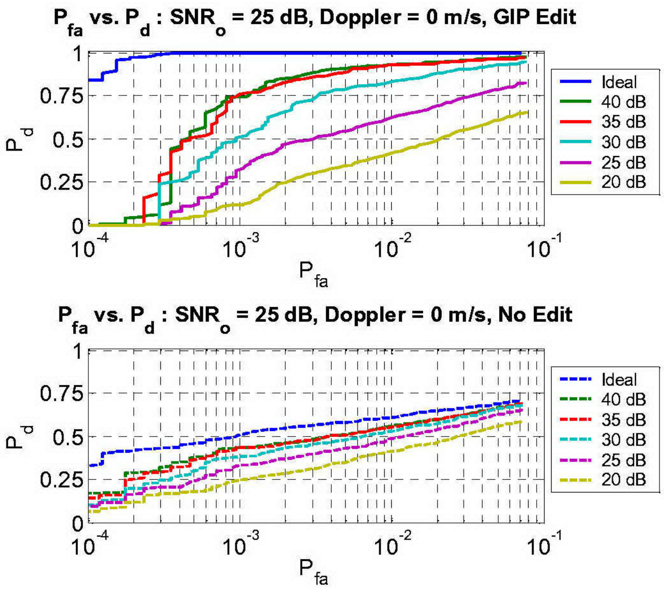

Fig. 5. P_d vs. P_{fa} curves for Doppler velocity 0 m/s with PD5. Unedited and GIP-edited results for all LFM waveforms shown. Legends indicate waveform type/peak sidelobe level.

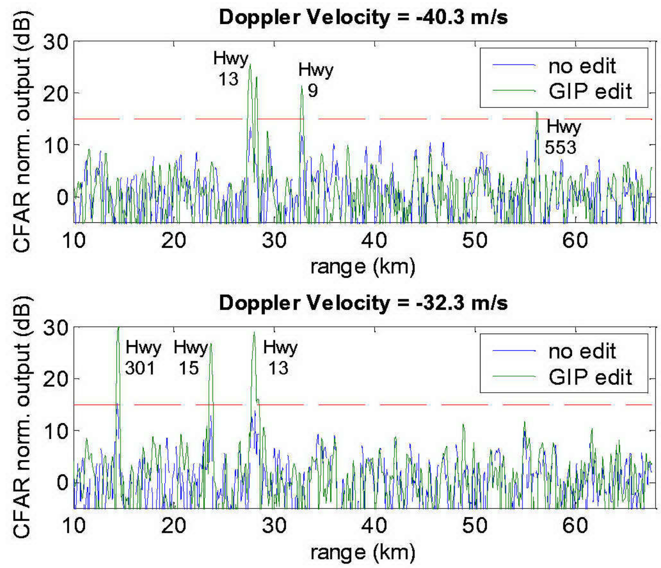

Fig. 6. Median CFAR processed beamformed output for the MCARM experimental data with both unedited and GIP-edited training data. A detection threshold of 15 dB and names of known roads close to the indicated detections also shown.

IV. MCARM Experimental Results

We now briefly summarize results of applying the GIP-editing method to the data from MCARM flight 5, Acquisition 575 [17]. Radar parameters for this L-band scenario may be found in [9]. The reduced-DoF 3-bin post-Doppler STAP implementation in conjunction with all 22 spatial elements was used to process the data. The covariance was estimated using twice the number of DoFs (i.e. 132 local training bins), 0 dB diagonal loading consistent with the estimated thermal noise level, and 2 guard bins. The data was pulse compressed using a 1 MHz LFM waveform.

Examination of the resulting rank-ordered GIP profiles at various Doppler velocities revealed the same central linear structure as found in the simulated data and predicted from theory. The multi-pass editing algorithm was applied with the fractional threshold parameter set to $\alpha = 0.25$.

The resulting GIP-edited training list, along with the unedited list, was used to perform STAP. Elsewhere, the improvement in SINR loss profiles as a function of Doppler velocity with GIP-editing over unedited training data was illustrated [15]. Median CFAR processed beamformed outputs at two Dopplers (-40.3 and -32.3 m/s; clutter at -12 m/s) where significant improvement in SINR loss was previously found are presented in Figure 6. A threshold of 15 dB was used to denote detections. At both Dopplers, the GIP-edited results indicate detections that were not present in the unedited results. Although ground truth for the targets in the scenario was not available for comparison, we do note that these detections correspond in range to the indicated roads.

This median CFAR detection process, with a threshold of 15 dB, was applied to all processed Doppler bins and potential target detections were identified. Due to the absence of ground truth, the detections were further processed from range-Doppler to range-azimuth and ultimately latitude-longitude using the WGS84 Earth model [18]. They were then compared with locations of known roads (using TIGER/Line [19] data). It is reasonable to assume that detections located by this process that are close to roads are likely actual ground movers. Figure 7 presents the results of this analysis for both the unedited and GIP-edited training lists. First of all, the number of detections effectively doubled (from 69 to 134) with the use of GIP-editing. Next we note that the GIP-edited results shows greater concentration and density of targets around the roads than does the unedited results. We conclude that GIP-editing has improved performance for this scenario.

V. Conclusions

This paper presents an adaptive thresholding algorithm that can be straightforwardly used in conjunction with the multi-pass GIP-based editing method to eliminate non-homogeneities from the training data used for STAP applications. Implementations for both full- and reduced-DoF processing were presented. The algorithm exploits the fact that the rank-ordered GIP statistic has a broad, central linear region, the theoretical origin of which was described in this paper. The algorithm requires a single input parameter α the allowable fractional deviation from this linear region, to determine the thresholds for excision. Guidance for choosing this parameter is provided in terms of a function with the number of DoFs and desired level of statistical Type I error used as inputs.

Robustness and performance of the method was demonstrated by applying it to STAP implementations with varying number of DoFs and sample support as applied to both high-fidelity site-specific simulated data and experimental data.

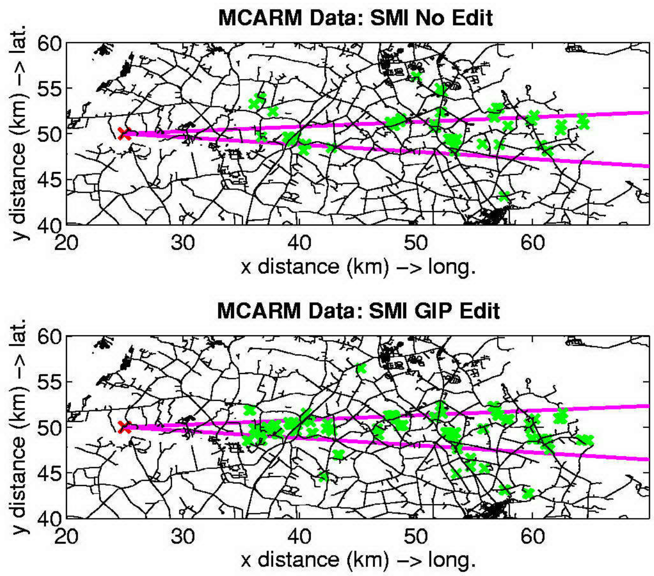

Fig. 7. MCARM detection results (x's) in relation to roads in the scenario. Top: No edit. Bottom: GIP edit. Detections increased from 69 to 134 with editing. Mainbeam of radar also shown.

STAP with GIP-edited training data was shown to have improved detection performance over unedited results for all cases. Editing performance was shown to degrade in the presence of LFM waveforms with increasing sidelobe levels but improvement over no-editing was still significant.

A preliminary analysis of computational complexity indicates that the most efficient way to implement the iterative editing process when using a local "sliding window" strategy [20] is to use a Cholesky factor up/down-dating scheme in the data domain, such as described in [21]. We note that if sufficient storage is available, the resulting converged Cholesky decomposition for each range bin from the GIP-editing process may be used in the subsequent data domain STAP step, thereby improving its efficiency.

Finally, since the number of contaminating targets in the training data naturally is reduced when lower sample support is used, we are also investigating ways of combining the GIP editing approach with methods that minimize sample support requirements such as knowledge-aided pre-whitening techniques [22].

REFERENCES

[1] J. Ward, "Space-time adaptive processing for airborne radar," Lincoln Laboratory Technical Report 1015, December, 1994.

[2] H. Wang and L. Cai, "On adaptive spatial-temporal processing for airborne surveillance radar systems," *IEEE Trans. on Aero. and Elec. Systems*, vol. 30, pp. 660-670, July, 1994.

[3] W. L. Melvin, M. C. Wicks, and R. D. Brown, "Assessment of multichannel airborne radar measurements for analysis and design of space-time processing architectures and algorithms," *Proc. of the 1996 IEEE National Radar Conference*, Ann Arbor, MI, May 13-16, 1996, pg. 130-135.

[4] W. L. Melvin and M. C. Wicks, "Improving practical space-time adaptive radar," *Proceedings of the 1997 IEEE Radar Conference*, Syracuse, NY, 1997, pg. 48-53.

[5] D. J. Rabideau and A. O. Steinhardt, "Improved adaptive clutter cancellation through data-adaptive training," *IEEE Trans. on Aero. and Elec. Sys.*, vol. 35, pp. 879-891, July, 1999.

[6] J. S. Bergin, P. M. Techau, W. L. Melvin, and J. R. Guerci, "GMTI STAP in target-rich environments: site-specific analysis," *Proc. of the 2002 IEEE Radar Conference*, Long Beach, CA, 22-25, April 2002.

[7] K. Gerlach, "Outlier resistant adaptive matched filtering," *IEEE Transactions on Aerospace and Electronic Systems*, vol. 38, pp. 885-901, July, 2002.

[8] M. Rangaswamy, B. Himed, and J. H. Michels, "Statistical analysis of the nonhomogeneity detector," *Proceedings of the 34th Asilomar Conference on Signals, Systems and Computers*, Pacific Grove, CA, November 2000, pg. 1117-1121.

[9] D. Sloper, D. Fenner, J. Arntz, E. Fogle, "Multi-channel airborne radar measurement (MCARM) flight test," Rome Lab. Final Technical Report, RL-TR-96-49, Vol. 1, April 1996.

[10] R. C. DiPietro, "Extended factored space-time processing for airborne radar systems," *Proceedings of the 26th Asilomar Conference on Signals, Systems and Computers*, Pacific Grove, CA, October 1992, pg. 425-430.

[11] KASSPER program website: http://www.darpa.mil/spo/programs/kassper.htm

[12] J. S. Bergin and P. M. Techau, "High-fidelity site-specific radar simulation: KASSPER '02 Workshop datacube," ISL Technical Report ISL-SCRD-TR-02-105, May 2002.

[13] H.A. David, *Order Statistics*, 2nd Ed., New York, Wiley,1981.

[14] M. Abramowitz and I. A. Stegun (Eds), *Handbook of Mathematical Functions with Formulas, Graphs and Mathematical Tables*, 9th Printing, New York: Dover, 1972.

[15] C. M. Teixeira, J. S. Bergin, and P. M. Techau, "Adaptive thresholding of non-homogeneity detection for STAP applications," *Proc. of the 2004 IEEE Radar Conference*, Philadelphia, PA, 24-26, April 2004.

[16] N. Levanon, "Detection loss due to interfering targets in ordered statistics CFAR," *IEEE Trans. on Aero. and Elec. Systems*, vol. 24, pp. 678-681, Nov. 1988.

[17] Provided by Dr. William Melvin of GTRI with the permission of the AFRL Rome Research Site.

[18] Department of Defense World Geodetic Systems 1984," NIMA Tech. Report TR8350.2, 3rd Ed., Amd. 1, Jan. 3, 2000.

[19] 1997 TIGER/Line ® File Technical Documentation, prepared by the Bureau of the Census, Washington, DC, 1997, http://www.census.gov/geo/www/tiger.

[20] G. K. Borsari and A. O. Steinhardt, "Cost-efficient training strategies for STAP algorithms," *Proceedings of the 29th Asilomar Conference on Signals, Systems and Computers*, Pacific Grove, CA, 30 Oct. - 2 Nov. 1995, pg. 650-654, vol. 1.

[21] C. M. Rader and A. O. Steinhardt, "Hyperbolic householder transformations," *IEEE Trans. on Acoust., Speech, Signal Processing*, vol. ASSP-34, pp. 1589-1602, Dec. 1986.

[22] J. S. Bergin, C. M. Teixeira, P. M. Techau, and J. R. Guerci, "Space-time beamforming with knowledge-aided constraints," *Proc. of the 11th ASAP Workshop, MIT Lincoln Laboratory*, Lexington MA, March 11-13, 2003.

Adaptive Thresholding of the GIP Statistic to Remove Ground Target Returns from the Training Data for STAP Applications

Twelfth Annual Workshop on
Adaptive Sensor Array Processing (ASAP)

16-18 March 2004

MIT Lincoln Laboratory

Christopher Teixeira
cmt@isl-inc.com

Jameson Bergin
jsb@isl-inc.com

Paul Techau
pmt@isl-inc.com

This work was sponsored by DARPA/IXO
under contract # DAAH01-02-C-R177

8130 Boone Blvd. Suite 500
Vienna, Virginia 22182
(703)448-1116   FAX: (703)356-3103
www.islinc.com

INFORMATION
SYSTEMS
LABORATORIES, INC.

Outline

- **Introduction**
  - Problem Illustration
  - Solution Approach Overview
  - Objectives
- **GIP-Based Editing**
- **Results**
- **Summary & Future Work**

Problem Illustration

- Ground moving detection performance with STAP is degraded due to inaccuracy of noise-plus-interference covariance estimate
- Two common sources of error due to use of training data are i) sample error, ii) target contamination

$$\frac{\text{SINR}}{\text{SNR}_0}$$

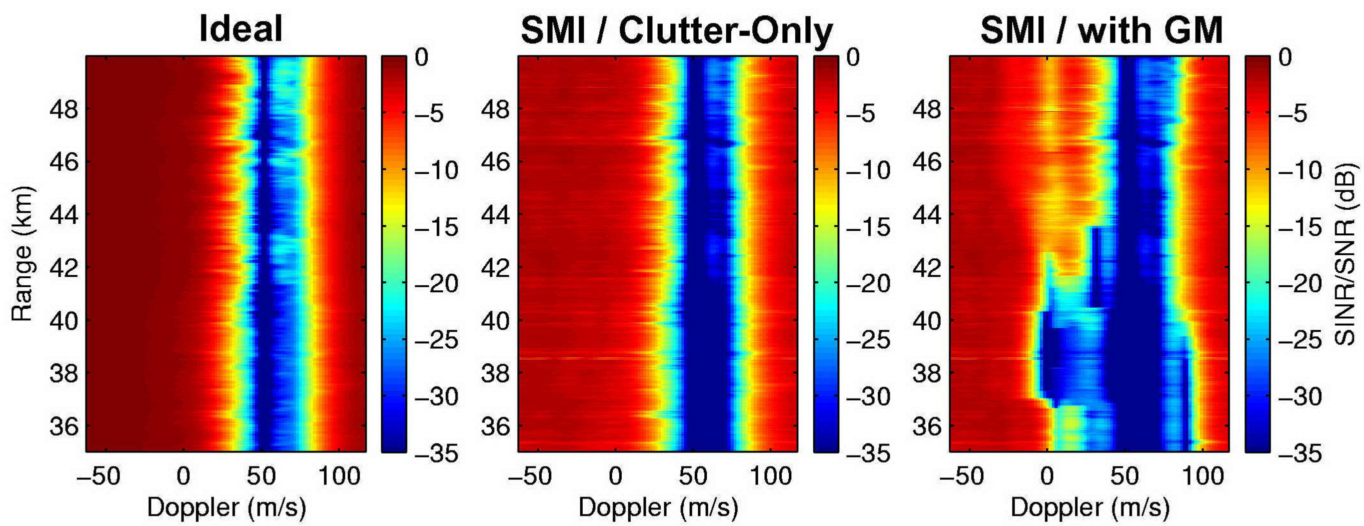

Pfa vs. Pd at 0 m/s

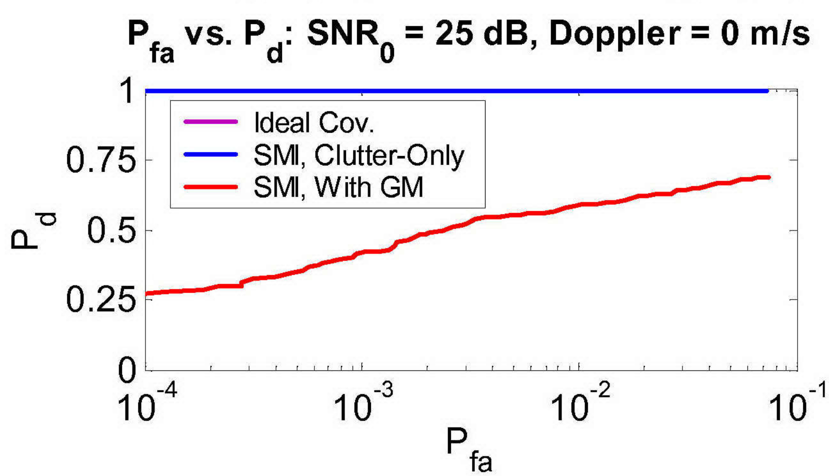

- Simulated L-band radar data
- Sample error widens clutter notch
- Target contamination results in nulls placed away from clutter
- Significantly degraded Pfa vs. Pd performance away from clutter may result

Solution Approach Overview

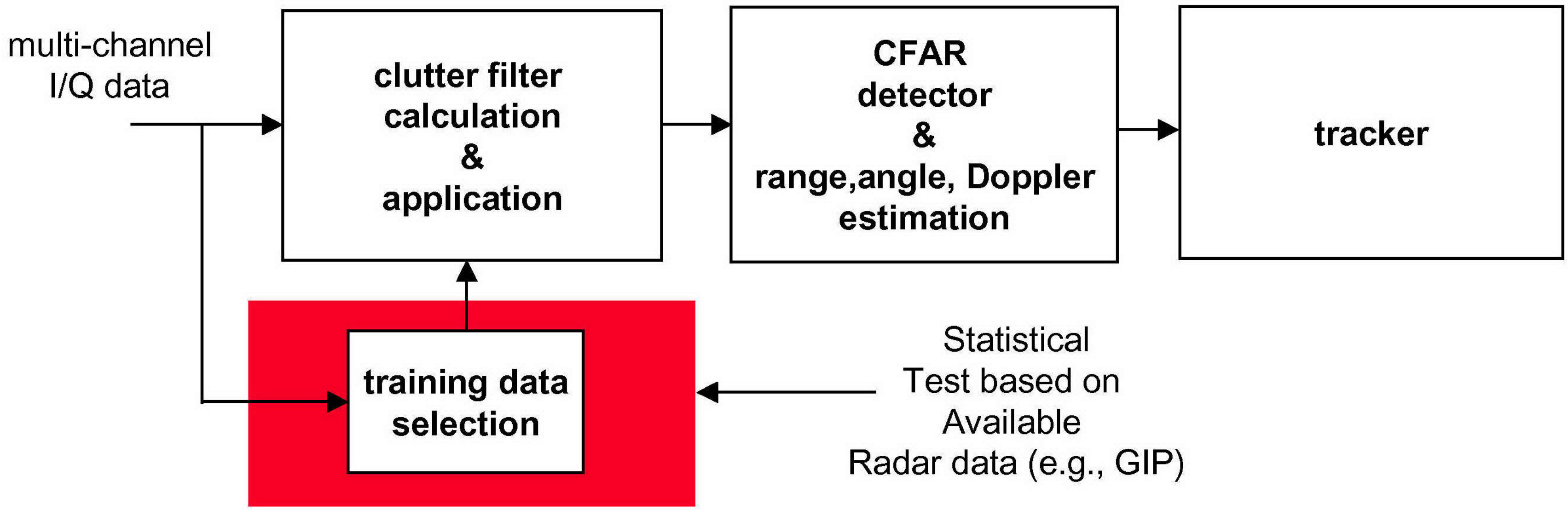

- **The goal is to remove training samples that contain ground targets from the training set**
- **Use multi-pass Generalized Inner-Product (GIP) test with adaptive thresholding to determine outliers which are then excised from the training data**
- **Use resulting edited training data to estimate noise+interference covariance matrix as required for adaptive clutter filter application**
- **Improved detection performance results**

Objectives

- Develop a practically implementable adaptive thresholding algorithm for use with the multi-pass GIP-based editing method
- Establish theoretical understanding and robustness of key features of algorithm
- Extend to reduced-DoF implementations
- Demonstrate performance improvement using GIP-based editing algorithms with STAP for broad range of operating environments and radar systems

Outline

- Introduction
- **GIP-Based Editing**
  - Definition
  - Illustration of Algorithm
  - Theory
- Results
- Summary & Future Work

Data-Dependent GIP-Based Editing

- **The Generalized Inner Product (GIP) statistic, γ, may be used to identify non-homogeneities in the data**

$$\gamma(k) = \mathbf{x}^H(k)\mathbf{R}^{-1}(k)\mathbf{x}(k) = \left|\mathbf{R}^{-1/2}\mathbf{x}\right|^2, \; k = \text{range bin}$$

x = data
R = clutter cov.

- **Outlier value of γ indicates that clutter-whitened data differs from noise; non-homogeneity present**

- **Works well when covariance estimate accurate (i.e. ideal covariance); distinction between noise and targets clear**

- **When GM contaminated training data used to estimate R, value of outlier γ reduced, makes detection much more difficult since distinction between noise/targets not as clear**

How to Determine Thresholds for Excision?

- **Remove prescribed number of bins; fix thresholds empirically**
  - **How to generalize/optimize ??**
- **Deterministic approaches based on ideal statistical properties**
  - **May be significantly in error due to practicality issues (e.g. non-stationary training data, loading of covariance estimate, etc.)**

Our Approach:

- **Analyze sorted GIP statistic, edit, iterate**
  - "Multi-pass GIP-editing"; [Melvin *et al*., RadarCon 96/97] and others
- **Apply adaptive thresholding to determine and excise outliers from training data**
  - Exploits characteristic structure of sorted GIP statistic
- **Iteration improves performance by enhancing distinction; typically converges < ~ 5 iterations**
- **Has been extended to reduced-DoF (e.g. multi-bin post-Doppler) STAP**
  - Perform editing using transformed data on per Doppler bin basis

Order-Based GIP Algorithm : L-band Example

- Ideal R result
- Large γ change when GM present
- Linear Fit to central region of sorted γ
- Adaptive limits shown (due to deviation from linear fit)
- $\alpha = 0.15$

- Sampled w/GM result
- Small γ change when GM present
- Same sorted structure as with Ideal R
- Adaptive limits shown (with same limit parameter, α)

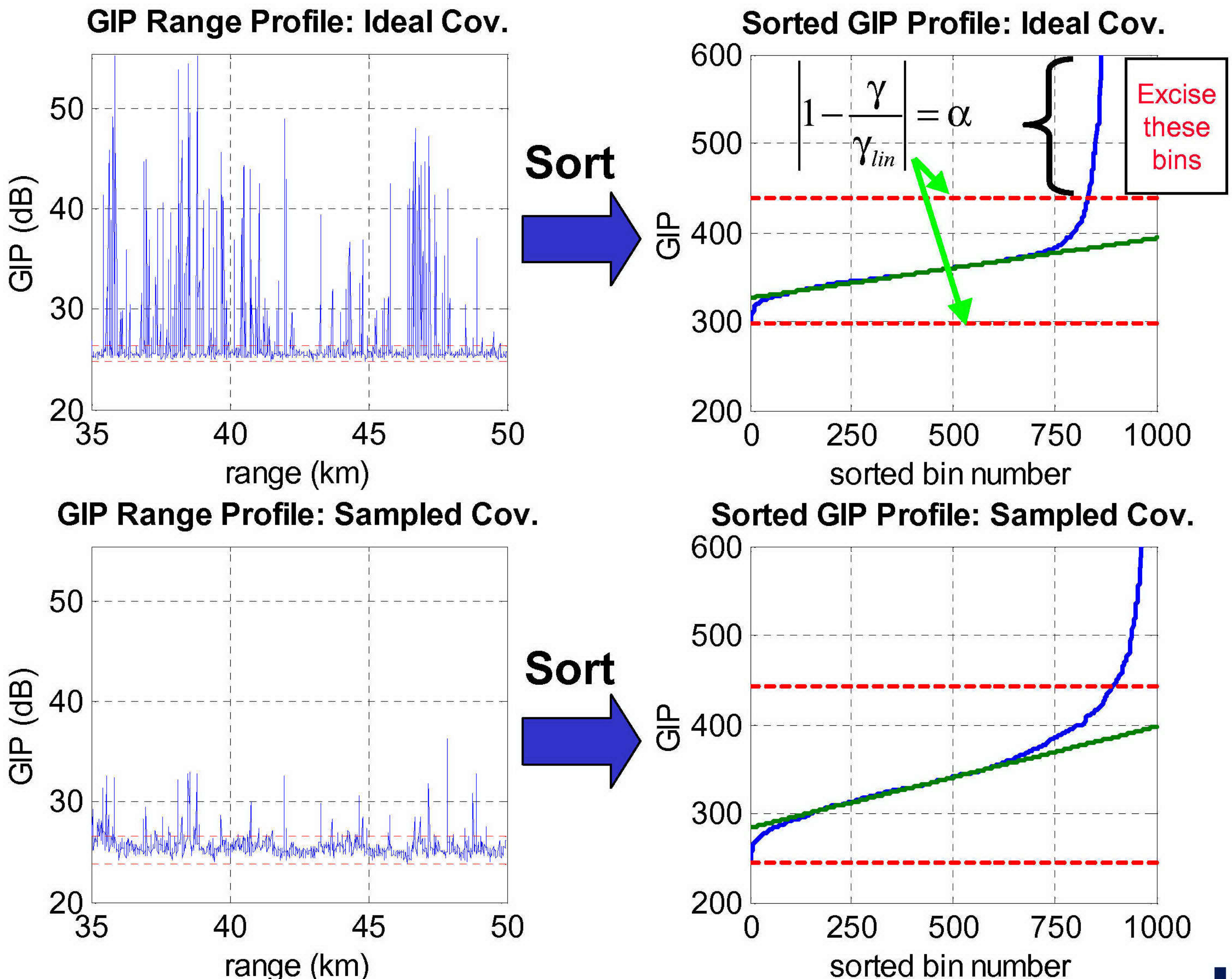

Summary of Theory of Rank-Ordered GIP

- **Existence of broad central linear region a consequence of the properties of the order statistics of the GIP**
  - The PDF of the *r*th ordered sample, out of *p* total, is well known**

- **The moments of the *r*th order statistic can be expressed in terms of the inverse of the GIP CDF, *F*, e.g. for the mean**

Beta PDF

$$\mu_r = \int_0^1 \left[F^{-1}(t)\right] f_\beta(t)\,dt$$

- **Assuming Gaussian data, exact expressions not available but possible to show that second order term in Taylor expansion of CDF around most probable value vanishes so that**

$$\mu_r \approx F^{-1}\left(\frac{r}{p+1}\right) \approx \sqrt{\frac{2\pi}{Q}}\left(\frac{r}{p+1}\right) + 1 - \sqrt{\frac{\pi}{2Q}} = \mu_{r,lin}$$

Q = # DoFs

- **Thus the mean of the *r*th ordered GIP statistic well approximated as linear function of normalized rank order around most probable value**

** H.A. David, *Order Statistics*, 1981.

Comparison of Theory to Simulated Data

- **Theory compared to single trial of GIP computed from L-band KASSPER data using the ideal covariance**
  - **In general non-Gaussian due to Internal Clutter Motion (ICM) model, heterogeneous terrain**

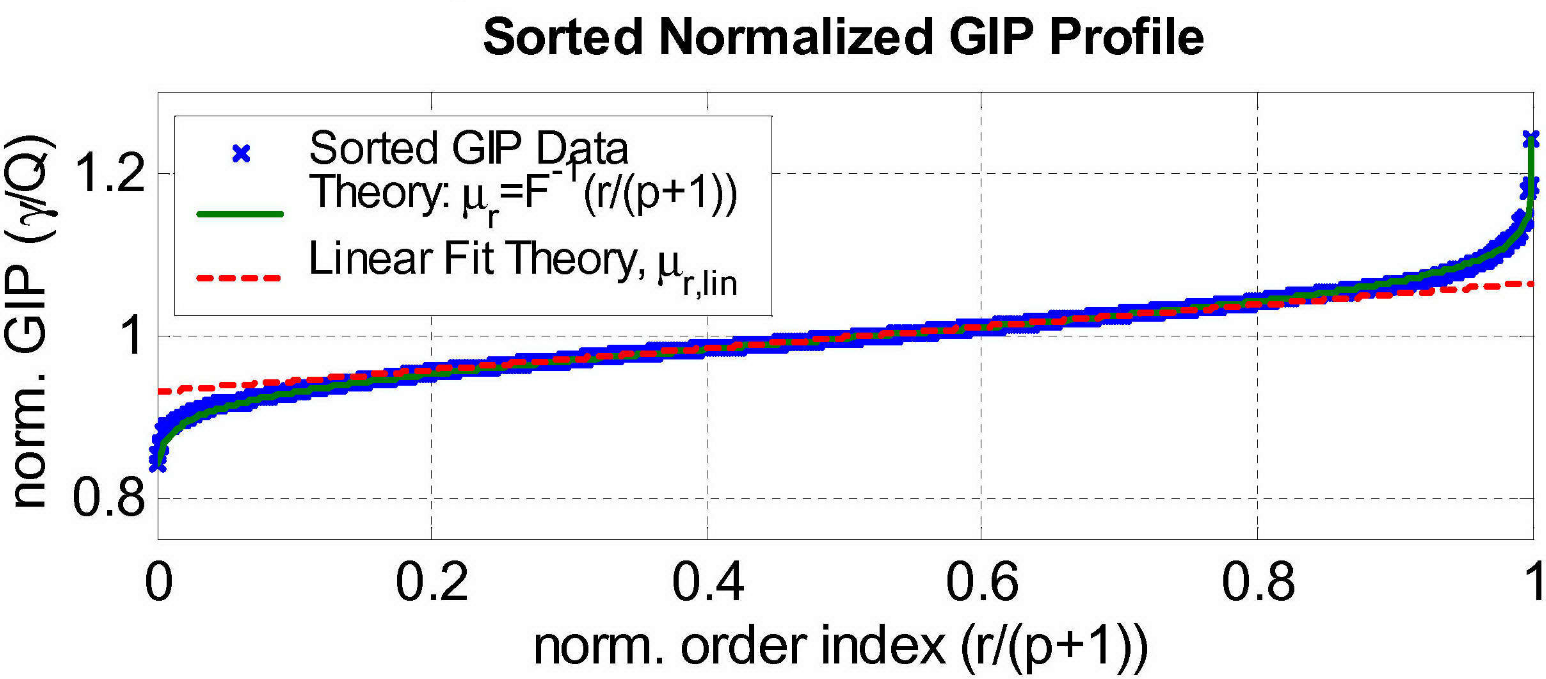

- **Extent of linear region and agreement with theory despite non-Gaussian nature of data indicates theory is somewhat robust**

Choice of Threshold Parameter, α

- GIP analysis suggests choice of α for given number of DoFs to achieve a desired Type I Error probability (i.e. probability of mistakenly editing out a range bin that is target-free)

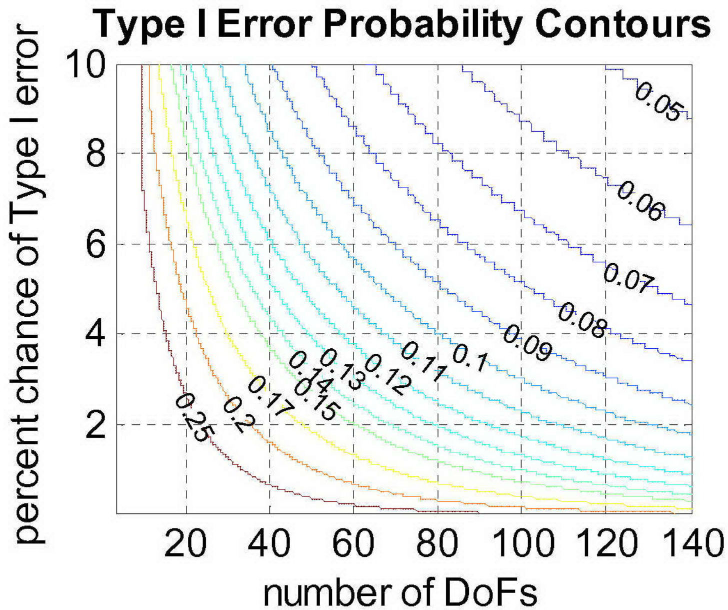

Contours of α

- For full-DoF simulations with # DoFs > 100 typically, α = 0.15 works well
- For reduced DoF (e.g. post-Doppler) should increase value of α to allow for greater variance of GIP ("fatter" tails)
- Use as guide for scenarios with non-stationary data

Outline

- Introduction
- GIP-Based Editing
- **Results**
  - High-Fidelity Site-Specific Simulated Data (KASSPER #1)
  - Experimental Data (MCARM)
- Summary & Future Work

First DARPA/AFRL KASSPER Scenario

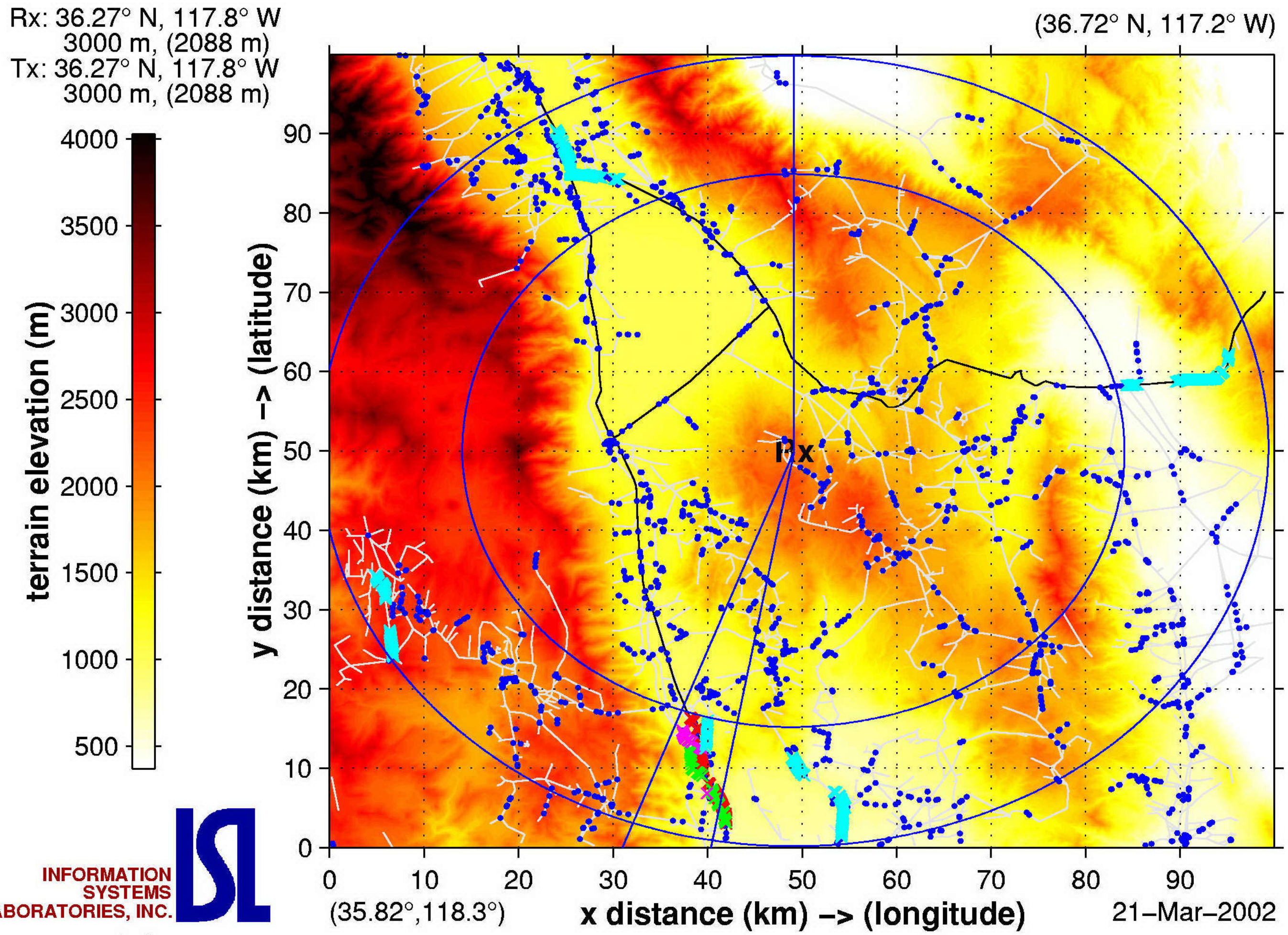

- **Mainbeam steering direction shown**
- **BW=10 MHz, PRF=1984 Hz, 11 subarray elements, 32 pulses; L-band**
- **Platform is heading west at 100 m/s and 3km altitude**
- **Range swath of interest shown**
- **About 200 targets in the mainbeam**
- **Array calibration errors, discretes included**
- **3 degree crab**
- **15 mph average wind speed (ICM)**

INFORMATION SYSTEMS LABORATORIES, INC.
www.islinc.com

Full-DoF Results : SINR Loss

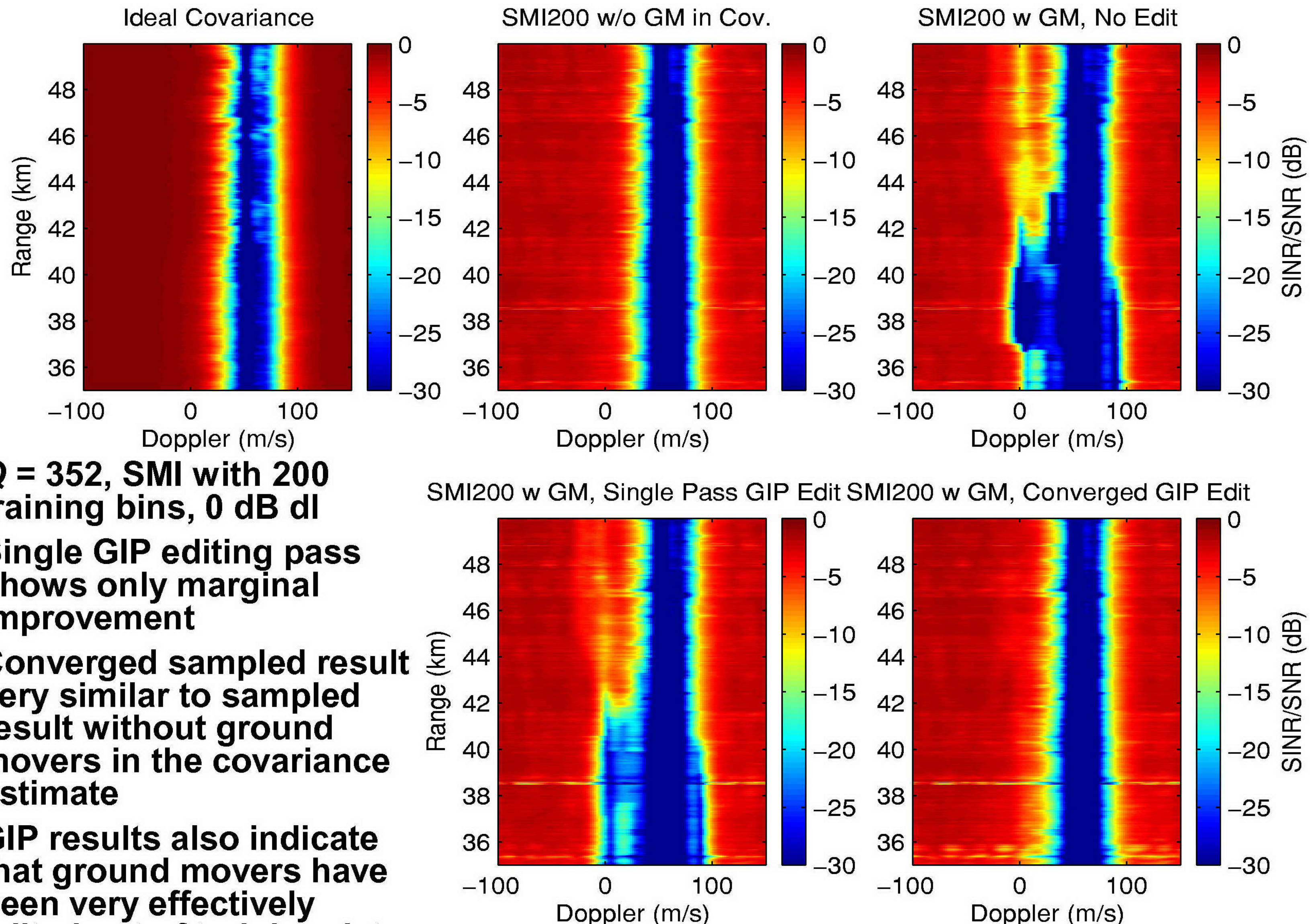

- ***Q*** **= 352, SMI with 200 training bins, 0 dB dl**
- **Single GIP editing pass shows only marginal improvement**
- **Converged sampled result very similar to sampled result without ground movers in the covariance estimate**
- **GIP results also indicate that ground movers have been very effectively edited out of training data**

Target Contaminated Range Bin Removal

Full-DoF

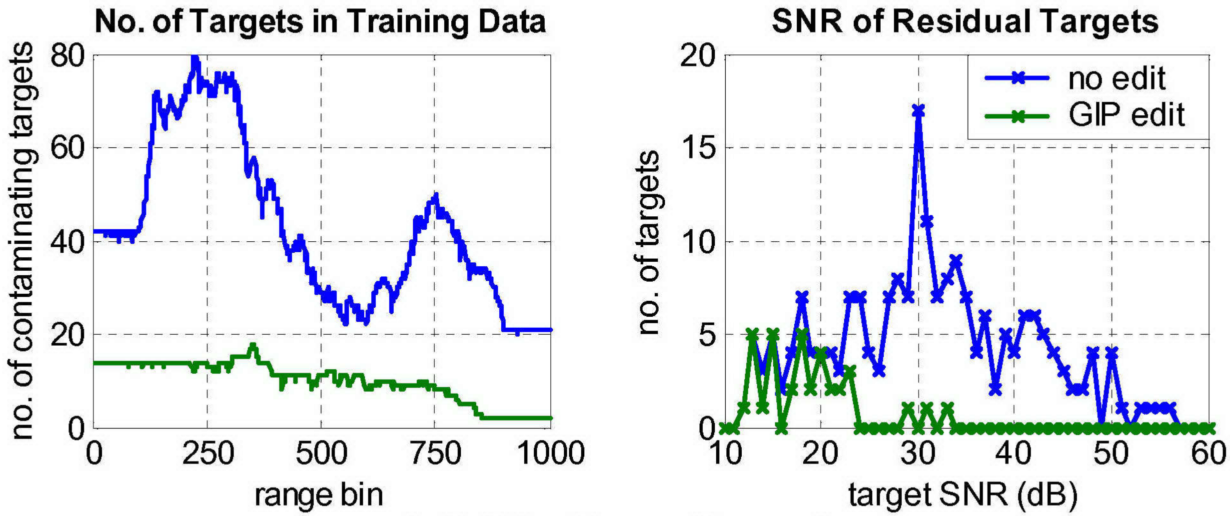

3,5-Bin Post-Doppler

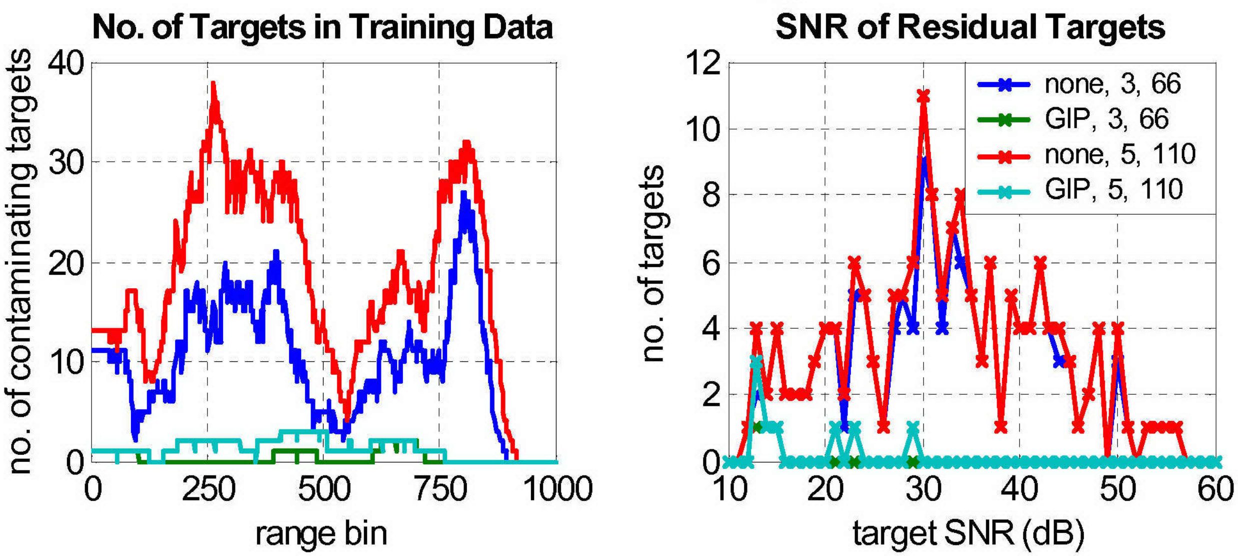

- **Extent of removal of target contaminated range bins from training data with GIP editing shown**
- **Scenario contains 206 detectable targets (SNR > 12 dB) within 169 range bins**
- **For Full DoF, 20-80 contaminating targets per range bin pre-editing; <18 after GIP editing**
- **Remaining targets tend to have low SNR**
- **Same trend with post-Doppler but fewer contaminating targets due to reduced sample support**
- **Very few low SNR targets remain after editing**

CFAR Detections: SMI without Editing

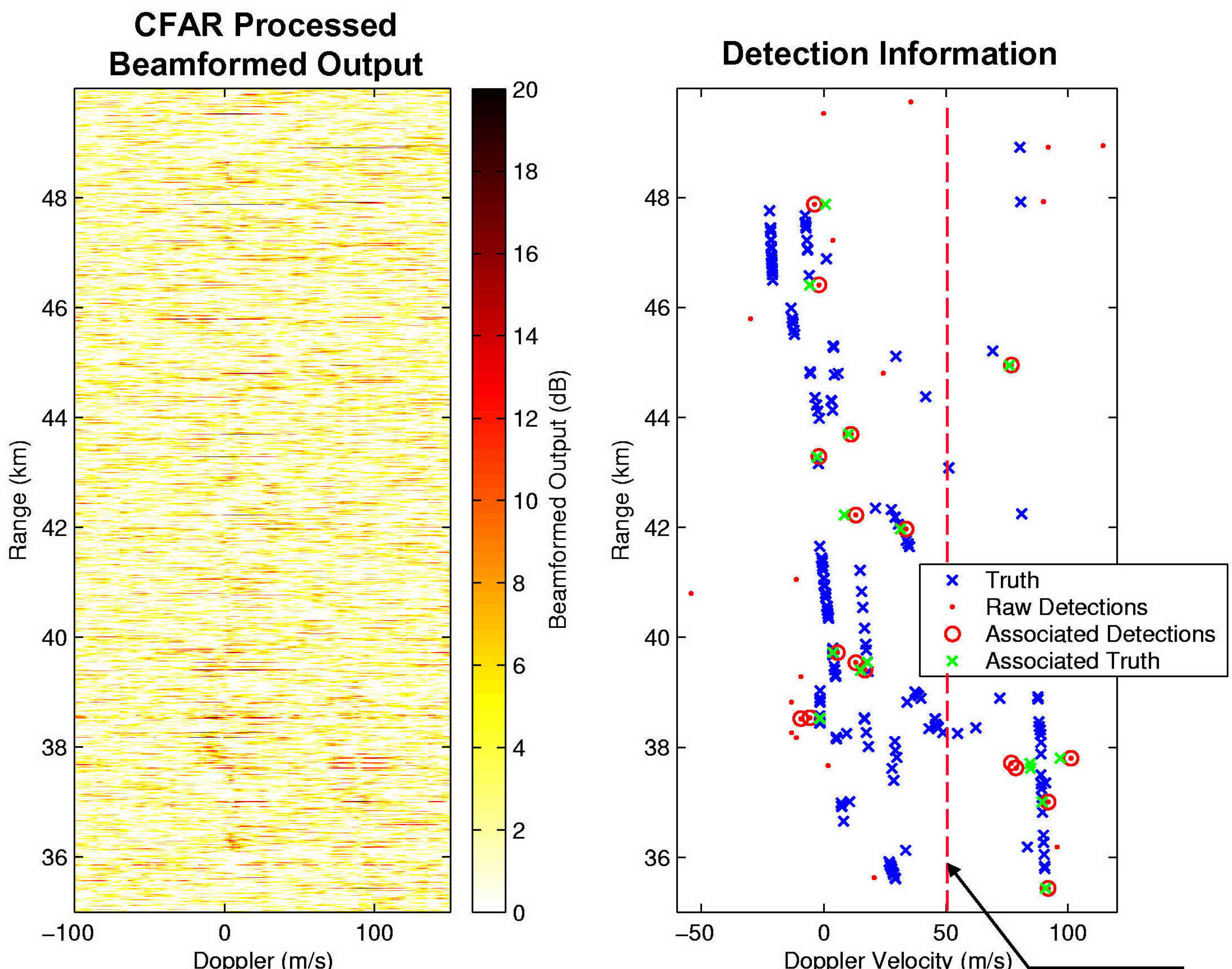

17 Associated Detections, 17 False Alarms

- **5-Bin post-Doppler STAP, K=110 + 0 dB dl**
- **Distortionless weights with median CFAR target detection**
- **Threshold = 13 dB; single detection per range bin**
- **Detected targets associated with ground truth when possible**
  - 40 m in range
  - 8 m/s in Doppler
- **Poor target detection due to target contamination**

CFAR Detections: SMI with GIP Editing

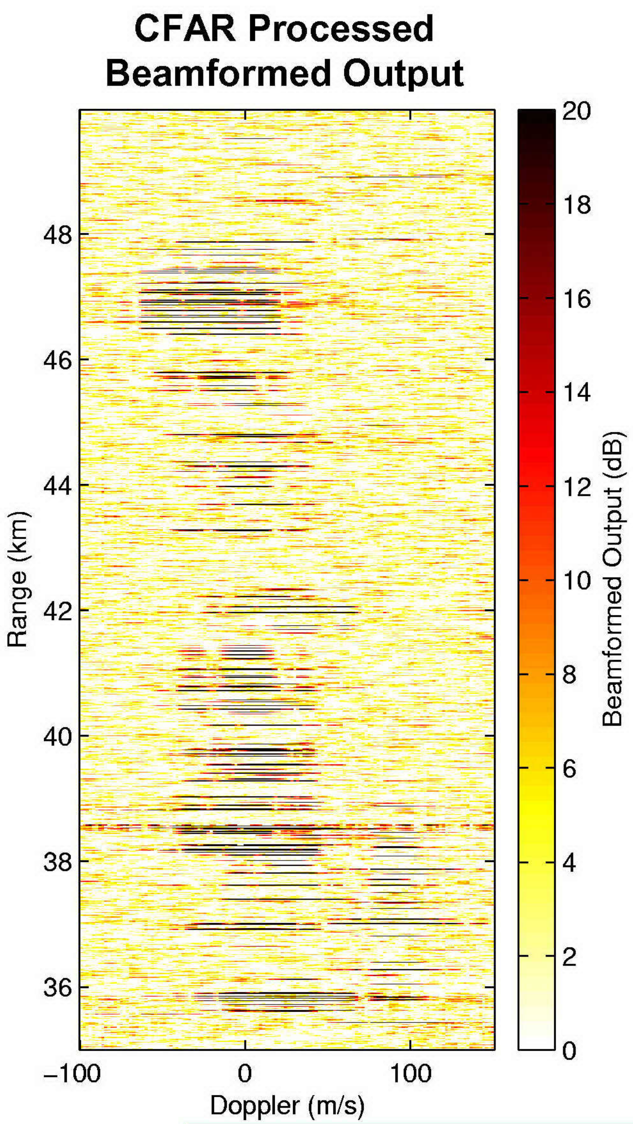

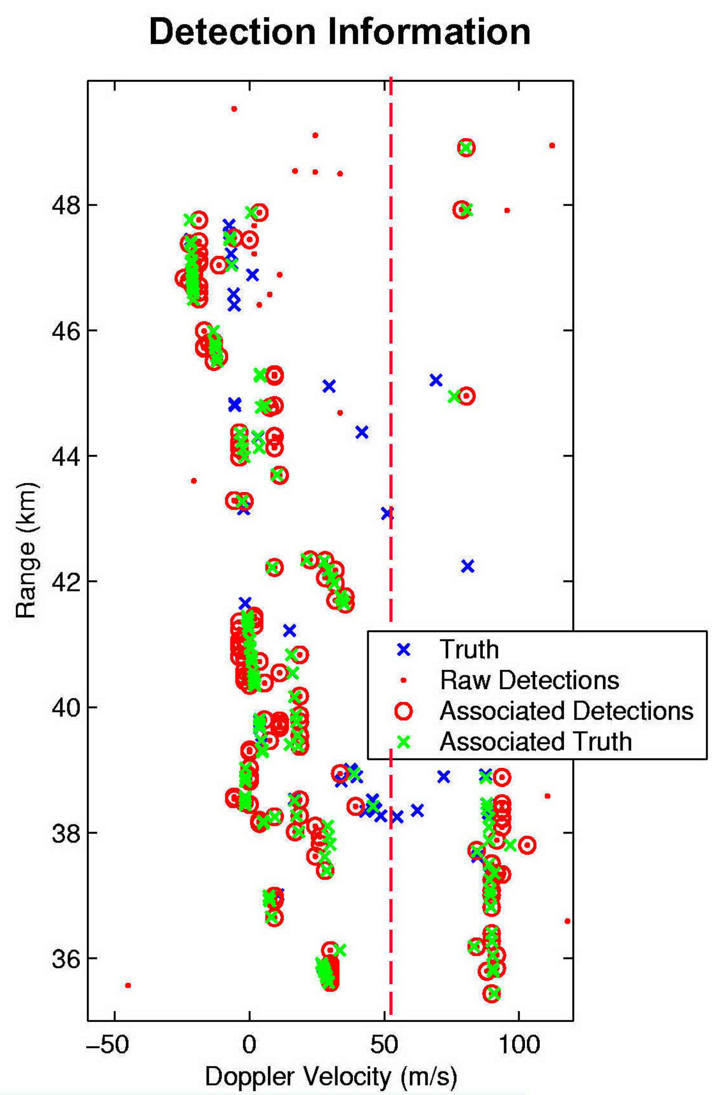

- Same STAP processing, CFAR detection process as in previous slide
- Dramatic improvement in number of associated detections due to GIP editing
- Comparable false alarm rate as with unedited results
- Clutter-Only SMI performance: 147 AD / 13 FA

143 Associated Detections, 22 False Alarms

Pd vs Pfa Performance : High Velocity Target

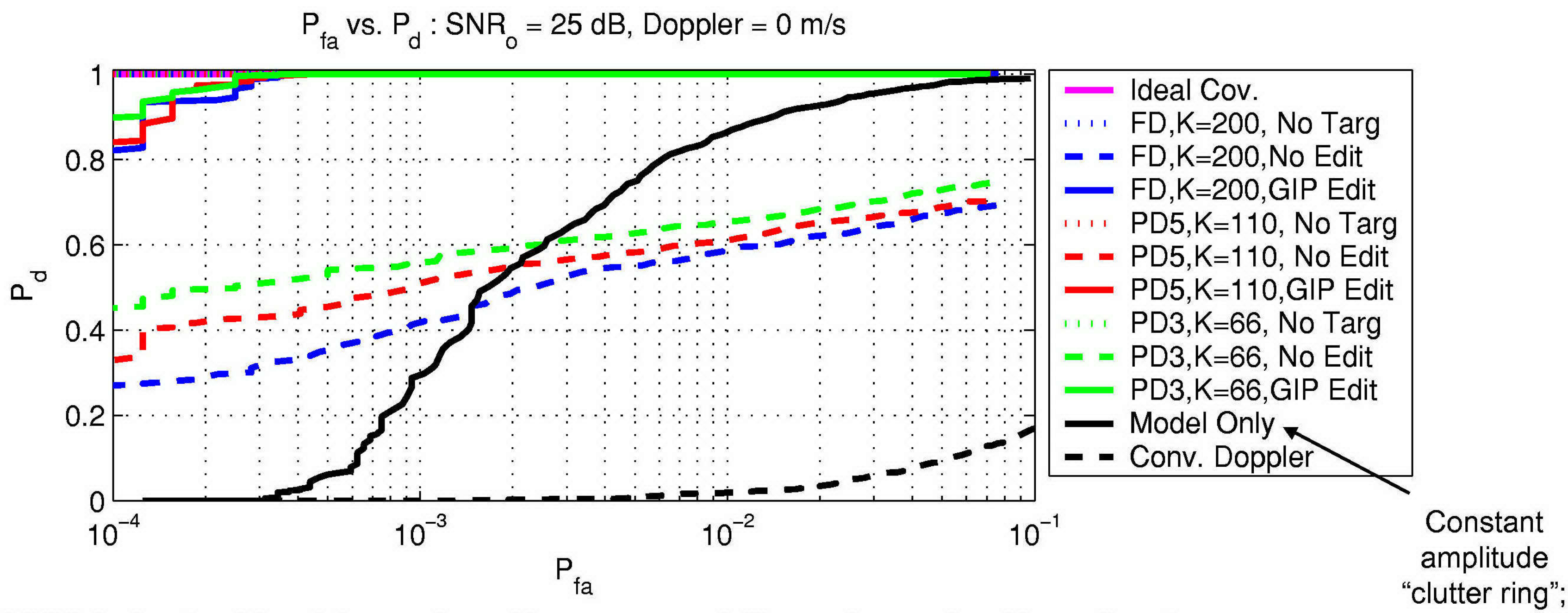

- **1000 injected test targets, all ranges, at Doppler velocity = 0 m/s (clutter at 51 m/s), target SNR is 25 dB at closest range bin (~ 5 dBsm)**
- **Detector includes median CFAR normalization of beamformed output prior to thresholding**
- **"No Targ" = no targets in training data (clutter-only);**
  "No Edit" = no editing of target contaminated training data;
  "GIP Edit" = GIP edited training data
- **No targets in CFAR training data for all cases**
- **GIP Editing recovers performance to close to clutter-only results**

Pd vs Pfa Performance : Low Velocity Target

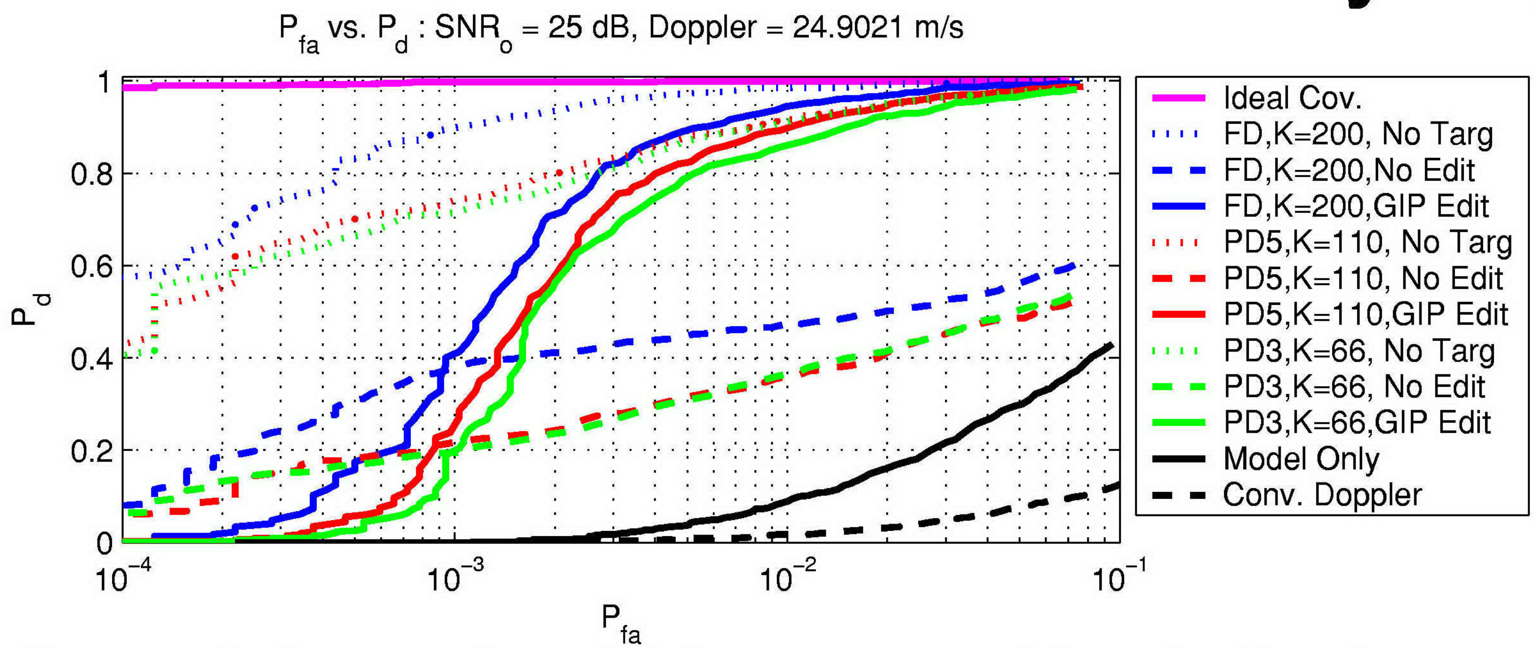

- **Same analysis as previous slide but targets now injected at Doppler velocity 24.9 m/s, which is closer to the clutter ridge (51 m/s)**
- **“No Targ” results show degradation due to sample estimation errors while “No Edit” results are further degraded due to target contamination**
- **“GIP Edit” results approach “No Targ” (clutter-only) performance as tolerable Pfa increases**
- **Loss of “GIP Edit” performance at low Pfa a result of wider spreading of training data over range leading to higher sample estimation errors due to terrain heterogeneity**
- **Examine if can be improved by combining with techniques that reduce sample support requirements (e.g. knowledge-aided pre-whitening)**

Experimental MCARM Scenario

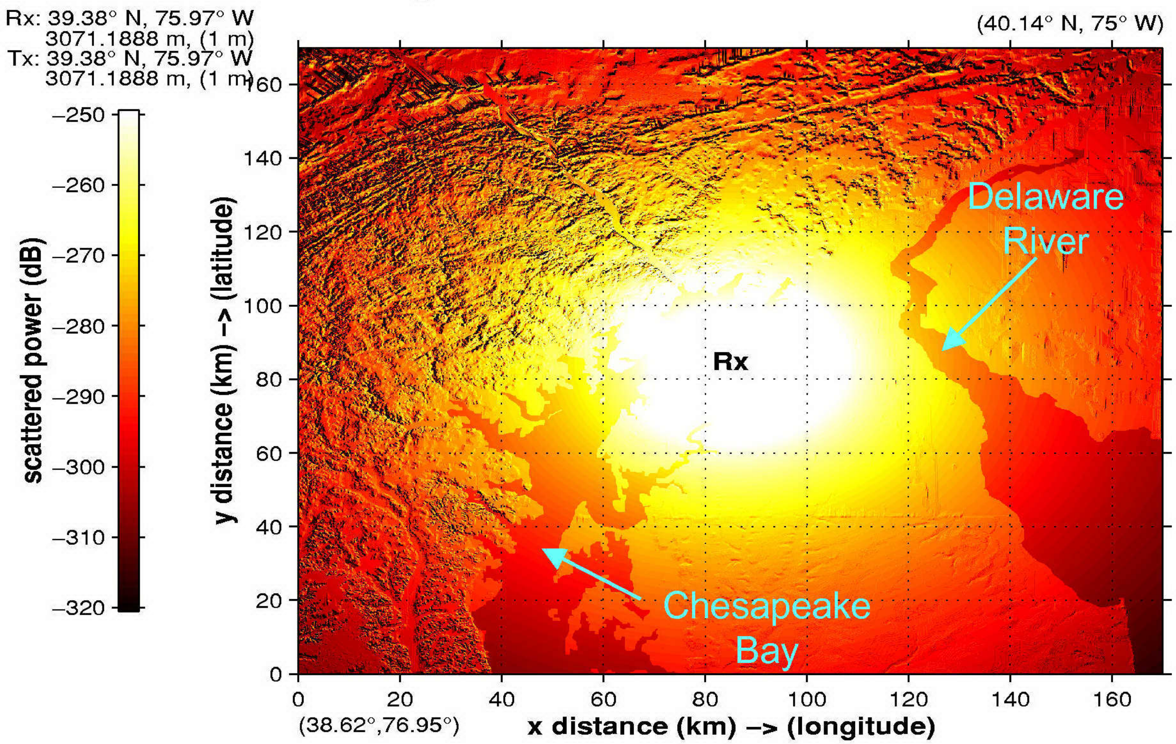

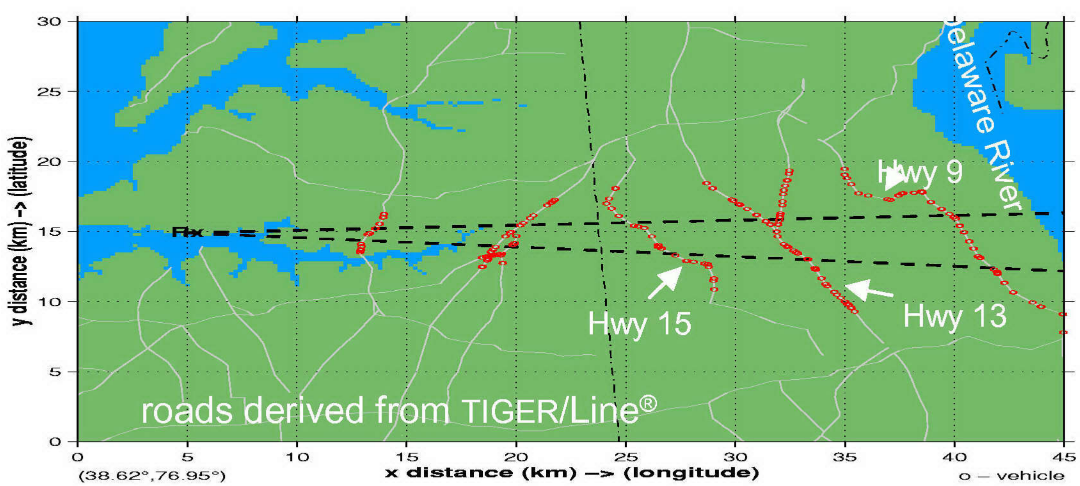

- Multi-Channel Airborne Radar Measurement (MCARM) scenario (Rome AFB RL-TR-96-49)
- Analyze MCARM Flight 5, Acquisition 575
- L-Band (1240 MHz)
- East of Baltimore, platform looking easterly
- PRF=1984 Hz, 2x11 channels, 128 pulses
- Many major roads intersecting mainbeam
- Low Bandwidth=0.8 MHz (~190 m range resolution, 346 bins)
- Typical GMTI radars use higher BW, range resolution
- Calibrated steering vectors provided
- Data is pulse compressed using 1 MHz LFM waveform

Experimental MCARM Data SINR Loss

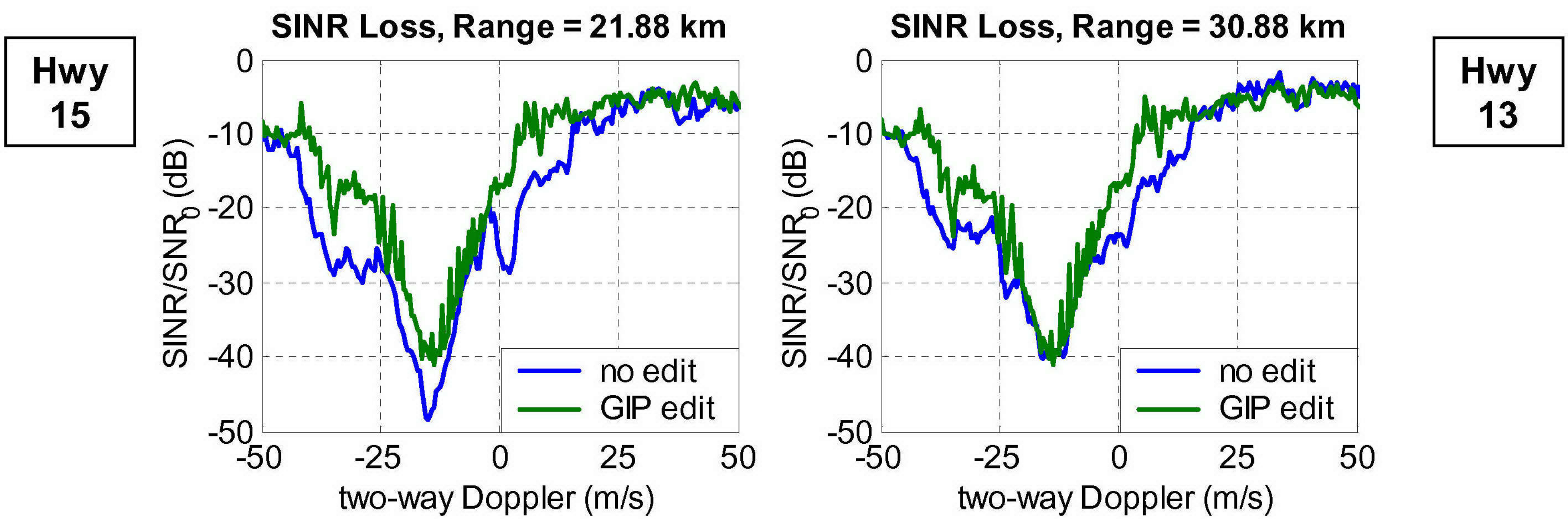

- **SINR Loss using 3-Bin post-Doppler with 2xDoF sample support (132 training bins) with 0 dB diagonal loading and 2 guard bins**
- **Results at ranges consistent with known roads**
- **Unedited and GIP-edited results shown**
- **Improvement with GIP approaches 13 dB for some Dopplers at shorter range, more moderate at longer range**
- **GIP-edit results indicate detections at ranges corresponding to known road locations not present with unedited results**

MCARM Experimental Detection Results

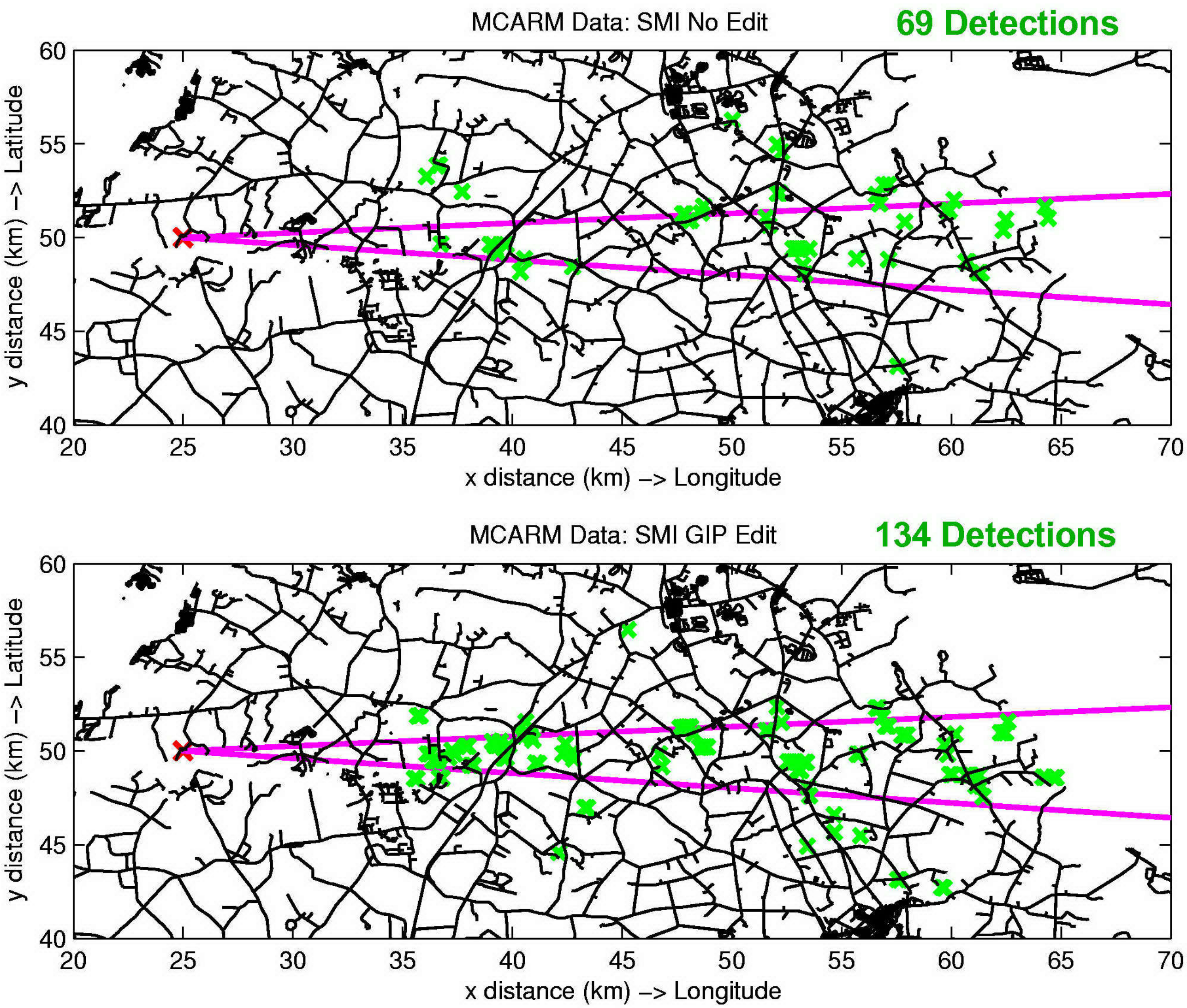

- **No ground truth**
  - Can't perform target association
- **Instead, find max response in azimuth for each target**
- **Convert from range-az to lat-lon and overlay roads**
  - Use TIGER/Line data and ISL's ellipsoidal Earth model toolkit
- **Top; No Edit: Bottom; GIP Edit**
- **Number of detections approx. doubled with GIP editing**
- **GIP edited detections appear more clustered around major road locations**

Summary & Future Work

- **Adaptive thresholding algorithm for multi-pass GIP-editing has been developed and applied to both simulated and experimental data**
  - Theoretical understanding of key features of algorithm developed; robust
  - Applicable to full and reduced DoF STAP implementations
  - Practically implementable with limited *a priori* knowledge required
  - Simulations of other X- and L-band scenarios have also been analyzed
- **In high-fidelity simulations GIP editing demonstrated dramatic performance improvement over no-editing**
  - Effectively recover performance of clutter-only training data
- **Range sidelobes from use of LFM waveforms degrades GIP editing performance due to target desensitization but significant benefit over no-editing still achieved (see associated paper)**
- **MCARM experimental analysis demonstrated target detection performance improvement due to GIP-editing**
  - Apply to other experimental data sets, as available
- **Computational complexity assessment ongoing**
  - Updating using “sliding window” in data domain being examined to optimize efficiency / performance trade-off
- **Address platform-specific implementation issues**

BACK-UP SLIDES

Datacube with LFM Targets

- **Previous results with simulated data used an ideal waveform**
- **Similar analysis performed on datacube using a compressed LFM waveform (with a Taylor nbar=6 taper) for all targets in the scene (duty factor = 0.1)**
- **Perform sensitivity study to sidelobe level**

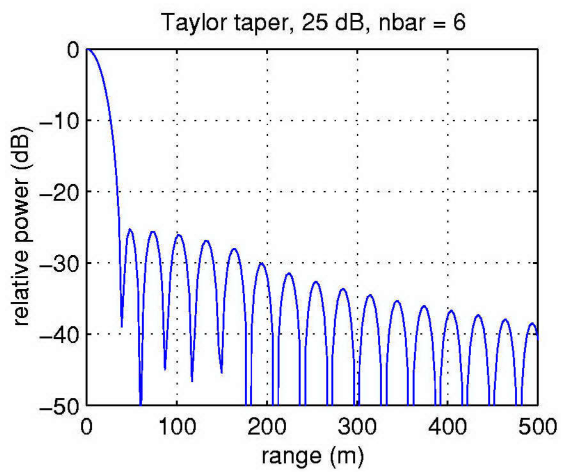

Compressed Targets

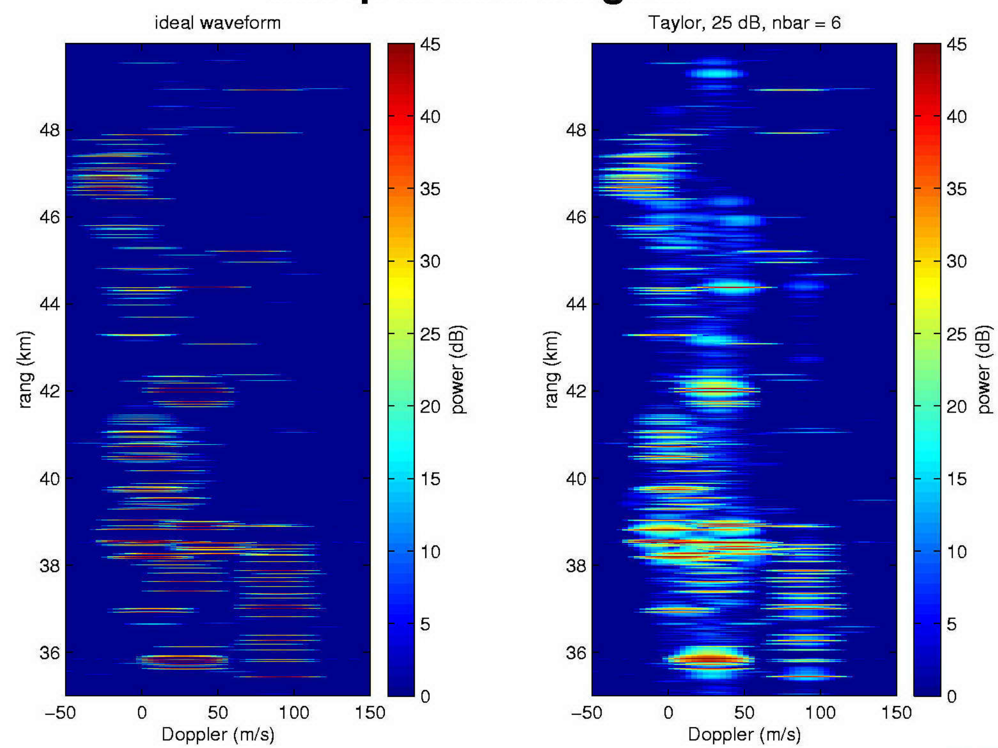

- **Produces range sidelobes from target returns**
- **Examine sidelobe levels of {20, 25, 30, 35, 40} dB**

Pd vs Pfa Performance with LFM

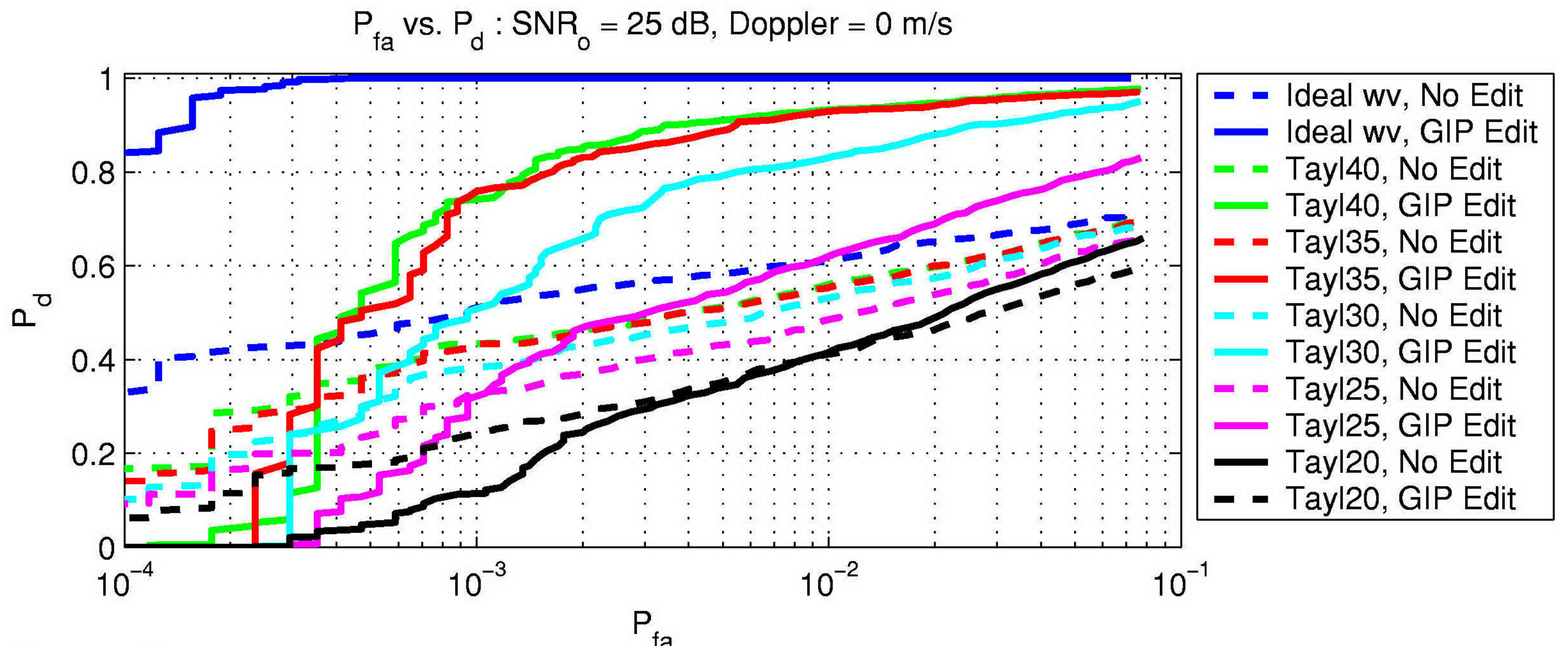

- **Same CFAR analysis as done previously, targets injected at Doppler velocity 0 m/s (clutter at 51 m/s)**
- **5-Bin post-Doppler with *K*=110 sample support, 0 dB diagonal loading**
- **Compare “No Edit” and “GIP Edit” performance for all waveforms**
- **Both “No Edit” and “GIP Edit” results degrade with increased sidelobe level**
- **Note comparable performance for 35 and 40 dB, consistent with SINR Loss results**
- **Except at largest sidelobe level (20 dB), GIP editing provides improvement in performance over no-editing with LFM waveform**